

1 Estimates of critical loads and exceedances of acidity and 2 nutrient nitrogen for mineral soils in Canada for 2014–2016 3 average annual sulphur and nitrogen atmospheric deposition

4
5 Hazel Cathcart¹, Julian Aherne², Michael D. Moran^{1*}, Verica Savic-Jovcic¹, Paul A. Makar¹, and
6 Amanda Cole¹.

7 ¹Air Quality Research Division, Atmospheric Science and Technology Directorate, Science and Technology Branch,
8 Environment and Climate Change Canada, Toronto, Ontario, M3H 5T4, Canada

9 ²School of the Environment, Trent University, Peterborough, Ontario, K9L 0G2, Canada

10 *Scientist emeritus

11
12 *Correspondence to:* Hazel Cathcart (hazel.cathcart@ec.gc.ca)

13 **Abstract.** The steady-state Simple Mass Balance model was applied to natural and semi-natural terrestrial
14 ecosystems across Canada to produce nation-wide critical loads of acidity (maximum sulphur, CL_{maxS} ; maximum
15 nitrogen, CL_{maxN} ; minimum nitrogen, CL_{minN}) and nutrient nitrogen (CL_{nutN}) at 250 m resolution. Parameterization
16 of the model for Canadian ecosystems was considered with attention to the selection of the chemical criterion for
17 damage at a site-specific resolution, with comparison between protection levels of 5% and 20% growth reduction
18 (approximating commonly chosen base-cation-to-aluminum ratios of 1 and 10 respectively). Other parameters
19 explored include modelled base cation deposition and site-specific nutrient and base cation uptake estimates based
20 on North American tree chemistry data and tree species and biomass maps. ~~Soil critical loads of nutrient nitrogen
21 were also mapped using the Simple Mass Balance model.~~ Critical loads of acidity were estimated to be low (e.g.,
22 below 500 eq⁻¹ ha yr⁻¹) for much of the country, particularly above 60°N latitude where base cation weathering rates
23 are low due to cold annual average temperature. Exceedances were mapped relative to annual sulphur and nitrogen
24 deposition averaged over 2014–2016. Results show that under a conservative estimate (5% protection level), 10%
25 of Canada's Protected and Conserved Areas in the study area experienced exceedance of some level of soil critical
26 load of acidity while 70% experienced exceedance of soil critical load of nutrient nitrogen.

27 1 Introduction

28 During the last three decades, reductions in sulphur (S) and nitrogen (N) ~~emissions and acidic~~ deposition have led to
29 improvements in ecosystem health across the U.S. and Canada; nonetheless, the acid rain question remains relevant
30 in Canada. Large point sources of emissions in western Canada have emerged, prompting concerns of impacts to
31 sensitive ecosystems in British Columbia and the Athabasca Oil Sands Region (AOSR) in northeastern Alberta (e.g.,
32 Mongeon et al., 2010; Williston et al., 2016; Makar et al., 2018). Further, increased marine traffic in the Arctic due
33 to the effects of anthropogenic warming has raised questions about potential impacts of acidic deposition on
34 northern ecosystems already under pressure from climate change (Forsius et al., 2010; Liang and Aherne, 2019).
35 Recovery of forest soils from decades of elevated acidic deposition in the northeastern U.S. and eastern Canada is

36 encouraging, but is predicted to be slow (Lawrence et al., 2015; Hazlett et al., 2020) and is complicated by the effect
37 of elevated N deposition (Clark et al., 2013; Simkin et al., 2016; Pardo et al., 2019; Wilkins et al., 2023) and climate
38 change (Wu and Driscoll, 2010). The importance of N deposition to acidification and eutrophication has received
39 increased recognition in recent years, prompting new avenues of risk assessment and mapping (e.g. empirical critical
40 loads of nitrogen; (Bobbink et al., 2022; Bobbink and Hicks, 2014). While N oxide emissions in Canada declined
41 by 41% between 1990 and 2022, ammonia emissions increased by 24% in that same period (ECCC, 2024).

42
43 The critical loads concept, defined as “the maximum deposition that will not cause chemical changes leading to
44 long-term harmful effects on ecosystem structure and function” (Nilsson and Grenfelt, 1988) is the primary tool for
45 identifying ecosystems that are sensitive to air pollution, particularly with respect to acidification and eutrophication
46 (De Vries et al., 2015; Burns et al., 2008). Ecosystems that receive ~~acidic~~ deposition above their critical load are
47 said to be in exceedance; that is, they are at risk of undergoing biological damage. Soil acidification is characterized
48 by attrition of base cations and a decrease in soil pH, which in turn causes leaching of toxic metals, such as
49 aluminum, and damage to plant roots. During the past three decades, these effects have been observed in forest soils
50 in the northeastern U.S. and eastern Canada (e.g., Cronan and Schofield, 1990; Likens et al., 1996; Lawrence et al.,
51 1999) that received acidic deposition in excess of their critical loads. The effects of nutrient N on ecosystems,
52 which include eutrophication, reduced plant biodiversity, and plant community changes, have also become an
53 emerging issue, with studies suggesting that some Canadian ecosystems are in exceedance of their nutrient N critical
54 load (e.g., Aherne and Posch, 2013; Reinds et al., 2015; Williston et al., 2016).

55
56 The standard approach for estimating soil critical loads is the Simple Mass Balance (SMB) model (Sverdrup and De
57 Vries, 1994, Posch et al., 2015), a steady-state soil chemistry model with several simplifying assumptions to reduce
58 input requirements. This approach has been used for regional and provincial critical load assessments in Canada
59 (e.g., Ouimet et al., 2006; Aklilu et al., 2022) as well as on a multi-provincial (NEG-ECP, 2001; Carou et al., 2008;
60 Aherne and Posch, 2013) and national scale (Reinds et al., 2015). However, nationwide implementations of the
61 SMB model in Canada have been challenged by data paucity and ~~disharmony-incompatibility~~ across provinces (i.e.
62 different data sources, methodology and spatial alignment), coarse input map resolution, and computational
63 difficulties driven by the size of the country and the subsequent size of data files used in critical load calculations.
64 In recent years, though, high-resolution input data (for soils, meteorology, and forest composition) have become
65 available and present an opportunity to refine, expand, and harmonise critical loads across the entire country,
66 including extending maps into the Canadian Arctic. These developments come at a time when policymakers in
67 Canada are seeking to define and track air quality impacts (such as those by acidic S and N deposition) on sensitive
68 ecosystems under the Addressing Air Pollution Horizontal Initiative (ECCC, 2021). Furthermore, development of
69 high-resolution critical loads of nutrient N to assess terrestrial eutrophication risk may contribute to efforts to meet
70 biodiversity goals such as those under the Kunming-Montreal Global Biodiversity Framework (ECCC, 2023c).
71 While the SMB model is a well-established and widely used approach to determine critical loads, there remains a

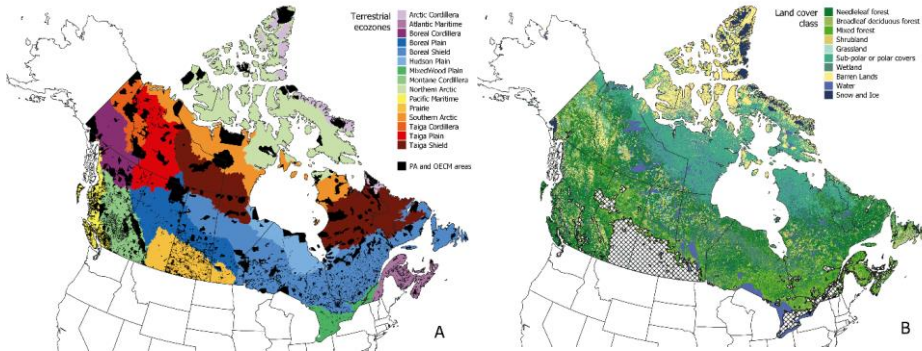
72 need for harmonised application across Canadian ecosystems to provide maps from which the effects of S and N
73 deposition can be ~~estimated~~assessed.

74
75 The objective of this study was to assess the impacts of acidic (~~S and N~~) and nutrient N deposition on terrestrial
76 ecosystems Canada-wide using the critical loads framework. In doing so, we applied a harmonised methodology to
77 the SMB model for Canadian ecosystems using high-resolution input maps, including modelled Canada-wide base
78 cation deposition (crucial for the estimation of critical loads). We also explored the choice of chemical (damage)
79 ~~eriterion-criteria~~ for Canadian ecosystems using a site-specific approach. Finally, we assessed the impact of
80 anthropogenic base cation deposition on exceedance estimates under annual average S and N deposition (ECCC,
81 2023a) for the three-year period 2014–2016, using the Canadian Protected and Conserved Areas Database (CPCAD;
82 ECCC, 2023b), to evaluate risk to sites that may be of interest to policymakers.

83 2 Methods

84 2.1 Study area

85 As the second-largest country by landmass in the world at over 9.9 million km², Canada is home to a variety of
86 climates, soils, vegetation, and geological structures that are ~~often~~-grouped into distinct ecozones ~~which are often~~
87 ~~used to generalise critical loads across similar ecosystems~~ (Figure 1A). The full extent of Canada was included in
88 this study to bring together estimates for all 10 provinces and 3 territories. However, only natural and semi-natural
89 soils meeting certain criteria for critical load estimations were considered. A land cover map (CEC, 2018) was used
90 to exclude non-soil ecosystems including water, wetlands, and permanent snow and ice (see Figure 1B). Soils were
91 further limited to natural and semi-natural ecosystems by excluding urban areas, crop classes, and areas within the
92 boundaries of the agricultural ecumene (Figure 1B). ~~Areas considered “barren” by land classification were not~~
93 ~~excluded when mineral soil depth was indicated in the interest of including as much of the Arctic region as possible;~~
94 ~~as the Arctic may be greening under global climate change (Myers-Smith et al., 2020) and northern shipping routes~~
95 ~~become viable, the question of ecosystem health in this region becomes more material.~~Areas considered “barren” by
96 ~~land classification were not excluded when soil depth was indicated.~~ Since peat and wetland soil classification is
97 difficult at a Canada-wide scale (i.e., data at the required scale are presently unavailable), and given that the satellite
98 land cover map underestimates wetland cover (3.7% versus an expected 13% as given by the National Wetlands
99 Working Group; 1997), organic soils with 30% or more organic matter content were filtered out to close this
100 gap. ~~Since peat and wetland soil classification is difficult at a Canada wide scale (i.e. data at the required scale are~~
101 ~~presently unavailable), organic soils with 30% or more organic matter content were filtered out.~~ The Hudson Plain
102 ecozone, which contains the world’s largest contiguous wetland and is 80% wetland by cover (ECCC, 2016), was
103 also broadly excluded from the study because of low mineral soil presence. ~~The Hudson Plain ecozone (which~~
104 ~~contains the world’s largest contiguous wetland) was also broadly excluded from the study because of very low~~
105 mineral soil coverage.

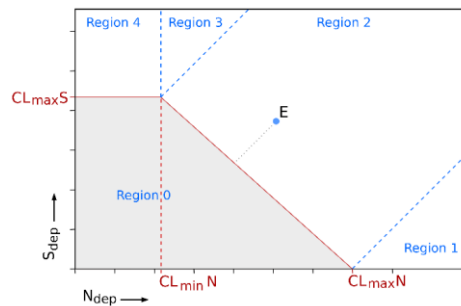


106 Figure 1: Study area illustrating the 15 terrestrial eozones of Canada (A, data source: Agriculture and Agri-Food
 107 Canada, 2013) with terrestrial Protected and Other Effective area-based Conservation Measures (OECM) areas in black
 108 (ECCC, 2023b), as well as 15 (compressed to 9 for visualisation) land cover classes (B, data source: CEC, 2018) with
 109 agricultural regions in crosshatch (Statistics Canada, 2017).

110

111 2.2 The Simple Mass Balance model for acidity and nutrient nitrogen

112 Critical loads of acidity were estimated using the SMB model, which balances sources, sinks, and outflows of S and
 113 N in terrestrial ecosystems while assuming ecosystems are at long-term equilibrium (i.e. about 100 years,
 114 representing at least one forest rotation cycle) (CLR TAP, 2015). The SMB model defines the critical load of S and
 115 N acidity (Figure 2) as a function of the maximum S critical load (CL_{maxS}), the maximum N critical load (CL_{maxN}),
 116 and the amount of N taken up by the ecosystem (CL_{minN}). Pairs of S and N deposition that fall outside this function
 117 (white region area, Figure 2) signify that the receiving ecosystem is in exceedance of its critical load of acidity (i.e.,
 118 it receives a potentially damaging amount of acidic deposition). Exceedance calculations are divided into four
 119 regions to determine the shortest path to the critical load line along the function:-



120

121 Figure 2: The acidity critical load function (red line) is defined by the maximum sulphur critical load (CL_{maxS}), the
 122 maximum nitrogen critical load (CL_{maxN}) and the minimum nitrogen critical load (CL_{minN}). Deposition points falling
 123 outside the critical load function (e.g., point E) are in exceedance (and defined as Regions 1-4), while those within the
 124 grey area (Region 0) are protected.

125 The determination of $CL_{max}S$ requires knowledge of non-sea salt base cation (calcium, magnesium, potassium,
 126 sodium) deposition (BC_{dep}), soil base cation weathering (BC_{we}), chloride deposition (Cl_{dep}), base cation uptake
 127 (BC_{up}), and the critical leaching of Acid Neutralizing Capacity (the ability of the ecosystem to buffer incoming
 128 acidity), denoted $ANC_{le,crit}$ (see Eq. 1). Note that sodium is included in some base cation terms (denoted BC , e.g.,
 129 BC_{we}) when sodium contributes to buffering, but where it concerns uptake by vegetation sodium is omitted since it is
 130 non-essential to plants (denoted Bc , e.g., Bc_{up}).

131

$$132 \quad CL_{max}S = BC_{dep} + BC_{we} - Cl_{dep} - BC_{up} - ANC_{le,crit} \quad \text{-----}$$

133 (1)

134

135 The value of $ANC_{le,crit}$ (see Eq. (2)) is determined from a critical base-cation-to-aluminum ratio (Bc/Al_{crit}), which is
 136 set to protect the chosen biota within ecosystems of interest (i.e., the critical chemical criterion), soil percolation or
 137 runoff (Q), and the gibbsite equilibrium constant (K_{gibb} , see section 2.7).

138

$$139 \quad ANC_{le,crit} = -Q^{\frac{2}{3}} \cdot \left(1.5 \cdot \frac{BC_{dep} + BC_{we} - BC_{up}}{K_{gibb} \left(\frac{Bc}{Al} \right)_{crit}} \right)^{\frac{1}{3}} - \left(1.5 \cdot \frac{BC_{dep} + BC_{we} - BC_{up}}{\left(\frac{Bc}{Al} \right)_{crit}} \right) \quad (2)$$

140

141 The calculation of $CL_{min}N$ from Eq. (3) describes the limit above which N deposition becomes acidifying, where N_u
 142 denotes N taken up by vegetation and N_i denotes long-term net immobilization of N in the root zone of soils under
 143 steady state conditions. A value of 35.7 eq ha⁻¹ yr⁻¹ (0.5 kg N ha⁻¹ yr⁻¹) was used, based on estimates of annual N_i
 144 since the last glaciation by Rosen et al. (1992) and Johnson and Turner (2014) who recommended a range of 0.2 –
 145 0.5 kg N ha⁻¹ yr⁻¹ and 0.5 – 1 kg N ha⁻¹ yr⁻¹ respectively; the midpoint (0.5 kg N ha⁻¹ yr⁻¹) was taken as a
 146 compromise. A value of 35.714 eq ha⁻¹ yr⁻¹ (0.5 kg N ha⁻¹ yr⁻¹) was used, based on estimates of annual N_i , since the
 147 last glaciation by Rosen et al. (1992). Lastly, $CL_{max}N$ is estimated from Eq. (4) using $CL_{max}S$, $CL_{min}N$, and the soil
 148 denitrification (the loss of nitrate to nitrogen gas) factor (f_{de} , see section 2.10).

149

$$150 \quad CL_{min}N = N_i + N_u \quad , \quad (3)$$

151

$$152 \quad CL_{max}N = CL_{min}N + \frac{CL_{max}S}{1-f_{de}} \quad . \quad (4)$$

153

154 Equation (5) was used to estimate soil critical loads of nutrient N ($CL_{min}N$), wherein the acceptable inorganic N
 155 leaching limit, a value set to prevent harmful effects of nutrient N such as eutrophication, vegetation community
 156 changes, nutrient imbalances, and plant sensitivity to stressors, is set from acceptable N concentrations in soil
 157 solution ($[N]_{acc}$) multiplied by Q (CLRTAP 2015). The $[N]_{acc}$ was set to 0.0142 eq m⁻³ (0.2 mg N l⁻¹ in soil solution)
 158 for conifer forests and 0.0214 eq m⁻³ (0.3 mg N l⁻¹) for all other semi-natural vegetation, following the generalised

159 approach taken for the European critical loads database (Reinds et al., 2021) as values suggested in CLRTAP (2015)
 160 are often country-specific and do not extend to other regions or ecosystems.

161

$$162 \quad CL_{nut}N = N_t + N_{up} + \frac{Q^*[M]_{acc}}{1-f_{de}} \quad . \quad (5)$$

163 2.3 Data and mapping

164 Critical load estimates were calculated with the statistical programming language R [version 4.1.0](#) (R Core Team,
 165 2021) [and the Terra package](#) (Hijmans, 2022), wherein inputs (Table 1) to and outputs from the SMB model were
 166 represented by 250 m resolution raster maps. Alignment and projection in [the World Geodetic System \(WGS84\)](#)
 167 followed the layers sourced from the OpenLandMap.org project (i.e., Hengl (2018c, a, d, b); Hengl and Wheeler
 168 (2018) in Table 1), since they represented the majority of input (raster) data sources. Output maps were visualised
 169 using QGIS (QGIS Development Team, 2023) with accessible colour schemes (Tol, 2012). Acidity critical load
 170 components (CL_{maxS} , CL_{maxN} , CL_{minN}) and $CL_{nut}N$ were all mapped using equivalents of acidity (or nutrient
 171 nitrogen) per hectare per year ($\text{eq ha}^{-1} \text{yr}^{-1}$).

172

173 **Table 1: Data sources for input parameters to the SMB model and critical load exceedance calculation.**

Parameter	Units	Use	Original resolution	Source
Temperature				
Average annual air temperature (1981–2010)	°C	BC_{we}	250 m	McKenney et al., 2006
Soil				
Absolute depth to bedrock	cm	BC_{we}	250 m	Hengl, 2017
Organic carbon	$\times 5 \text{ g kg}^{-1}$	BC_{we}	250 m	Hengl & Wheeler, 2018
Sand fraction	%	BC_{we}	250 m	Hengl, 2018c
Clay fraction	%	BC_{we}	250 m	Hengl, 2018a
Bulk density	g/cm^3	BC_{we}	250 m	Hengl, 2018d
Coarse fragment volume	%	BC_{we}	250 m	Hengl, 2018b
Parent material acid class	class	BC_{we}	250 m	CLBBR, 1996; SLCWG, 2010
Drainage class	class	BC_{we}	250 m	CLBBR, 1996; SLCWG, 2010
Runoff (Q)	mm yr^{-1}	$ANC_{le,crit}$	$0.05^\circ \times 0.1^\circ$	Reinds et al., 2015
Vegetation				
Tree species composition	%	BC_{up} , N_{up}	250 m	Beaudoin et al., 2014
Biomass	Mg ha^{-1}	BC_{up} , N_{up}	250 m	Beaudoin et al., 2014
Harvestable boundaries	km^2	BC_{up} , N_{up}	250 m	Dymond et al., 2010
Tree chemistry database (U.S.)	% Ca, Mg, K, N	BC_{up} , N_{up}	-	Pardo et al., 2005
Tree chemistry database (Can.)	% Ca, Mg, K, N	BC_{up} , N_{up}	-	Paré et al., 2013
Land cover (2010)	class	Limiting extent	250 m	(CEC, 2018)

Agricultural ecumene (2016)	class	Limiting extent	5 km	Statistics Canada, 2017
Ecozones	class	Limiting extent, summary statistics	1:7.5 million	Agriculture and Agri-Food Canada, 2013
Deposition				
Base cation deposition (2010, 2016)	eq ha ⁻¹ yr ⁻¹	$ANC_{le,crit}$	12 km	{Galmarini et al., 2021}
Total mean S and N deposition (2014–2016)	eq ha ⁻¹ yr ⁻¹	Exceedance	10 km	{Moran et al., 2024b, a}
Canadian Protected and Conserved Areas Database	class	Identifying areas of special interest	Various	{ECCC, 2023b}

174

175 2.4 Base cation weathering

176 ~~Generalised~~ Base cation weathering BC_{we} (i.e., calcium, magnesium, potassium and sodium) was mapped using the
177 soil type–texture approximation method, which assigns a base cation weathering class (BC_{w0}) based on soil
178 characteristics (organic matter, sand, and clay percentage) and parent material acid class (see Eq. 6). [A temperature](#)
179 [correction was applied to the \$BC_{we}\$ as the speed of chemical weathering can be affected by temperature.](#) Weathering
180 is modified by ambient temperature T , where A is the Arrhenius pre-exponential factor (3600 K), a temperature
181 coefficient for soil weathering (de Vries et al., 1992; CLRTAP, 2015). [Note that average annual air temperature was](#)
182 [used to approximate annual average soil temperature in absence of a Canada-wide soil temperature map.](#) To address
183 issues with resolution and continuity across provinces, high-resolution (global 250 m) predicted soil maps from the
184 OpenLandMap.org project were used for the following input variables: bulk density (ρ), organic carbon, coarse
185 fragment volume (CF), and sand and clay composition (see Table 1). One of the assumptions of the SMB model is
186 that the soil compartment is homogeneous; therefore, a weighted average for soil texture was developed based on
187 layer depth, total depth (D), and corrections based on coarse fragment volume, percent organic matter, and bulk
188 density. Percent organic matter (OM) was obtained by dividing organic carbon (~~in $\times 5 \text{ g kg}^{-1}$~~) by 2 ([as](#)
189 [recommended by Hengl & Wheeler, 2018](#); Pribyl, 2010).

190

$$191 \quad BC_{we} = \left(\frac{\rho_{soil}}{\rho_{H_2O}} \right) D \left(1 - \frac{CF}{100} \right) \left(1 - \frac{OM}{100} \right) (BC_{w0} - 0.5) * 10^{\left(\frac{A}{281} - \frac{A}{273+T} \right)} \quad (6)$$

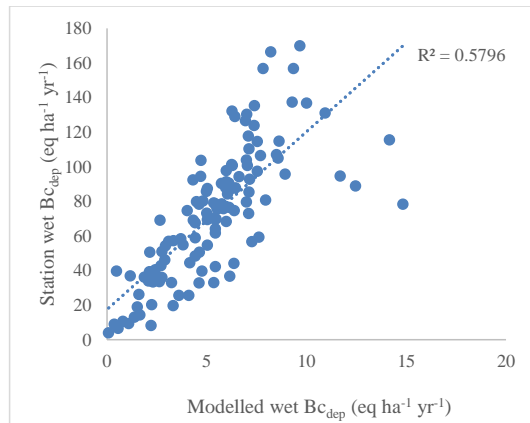
192

193 A second assumption is that the profile depth (D) is limited to the root zone, which was set to a maximum of 50 cm
194 for forest soils and 30 cm for other land cover types such as shrubland, grassland and tundra. Soil depth was further
195 limited by an absolute-depth-to-bedrock global modelled map (Hengl, 2017; Shangguan et al., 2017) in case bedrock
196 was < 50 cm. Base cation weathering omitting sodium (BC_{we}) required for the calculation of $ANC_{le,crit}$ (Eq. 2) was
197 scaled by 0.8 after CLRTAP (2015).

198 **2.5 Base cation deposition**

199 In the absence of modelled $Be_{dep}-BC_{dep}$ data, previous Canadian mapping studies have employed a single value, or
200 coarsely interpolated from limited Canadian Air and Precipitation Monitoring Network (CAPMoN) stations from
201 1994–1998 (Aklilu et al., 2022; Carou et al., 2008; Ouimet et al., 2006). Critical loads estimates for Canada by
202 Reinds et al. (2015) used coarse modelled global Ca deposition (Tegen and Fung, 1995) based on soil Ca content
203 (Bouwman et al., 2002) and estimated the other ions by regression. To address the gaps in data availability and
204 spatial distribution, $Be_{dep}-BC_{dep}$ in this study was sourced from modelled estimates produced with the Global
205 Environmental Multiscale–Modelling Air-quality and CHemistry (GEM-MACH) model at 12-km horizontal grid
206 spacing for the air quality multi-model comparison project AQMEII4 (Galmarini et al., 2021). Two different GEM-
207 MACH configurations, a version with detailed parameterizations and a second version with some simplified
208 parameterizations used for operational air-quality forecast simulations, estimated wet and dry non-sea-salt Be_{dep}
209 BC_{dep} for North America. Gridded annual deposition fields for two periods, 2010 and 2016, were obtained. Ideally,
210 emissions data sources used for S and N deposition and $Be_{dep}-BC_{dep}$ would be the same; however, $Be_{dep}-BC_{dep}$ is often
211 not evaluated, and the version of the emissions inventories used for S and N deposition did not include $Be_{dep}BC_{dep}$.
212 In the absence of a modelled Cl_{dep} map, and since the model estimates non-marine BC_{dep} , Cl_{dep} was assumed to equal
213 sodium deposition; BC_{dep} is therefore referred to as BC_{dep} . Comparison of modelled wet BC_{dep} to measured wet BC_{dep}
214 data from 33 Canadian Air and Precipitation Monitoring Network (CAPMoN) precipitation-chemistry stations (Feng
215 et al., 2021) and 87 U.S. National Atmospheric Deposition Monitoring (NADP) precipitation-chemistry stations
216 (NADP, 2023) within 300 km of the Canada-U.S. border showed that modelled BC_{dep} data were underestimated in
217 each model configuration and year by an average factor of 15, though the correlation was relatively high (Figure 3).
218 A BC_{dep} input map was prepared by averaging (wet plus dry) BC_{dep} across the two model runs and two years, scaling
219 up by 15 (after Figure 3), and resampling to the 250 m soil grid using bilinear interpolation.

220



221
 222 **Figure 3: Modelled annual wet non-sea salt $B_{c,dep}$ (Ca + Mg + K) versus measured annual $B_{c,dep}$ at CAPMoN and NADP**
 223 **stations (NADP stations limited to those within 300 m of the Canada-U.S. border). Values are averaged across two years**
 224 **(2010 and 2016) and two model configurations. Marine station sites were corrected for sea salt contributions.**

225 The modelled $B_{c,dep}$ and station observations include anthropogenic input, but the $B_{c,dep}$ input to the SMB model is
 226 meant to reflect long-term non-anthropogenic sources of base cations. However, large point sources of $B_{c,dep}$ (such as
 227 surface mines) are a feature of some Canadian regions, and their impact should not be overlooked in critical load
 228 assessments. The modelled $B_{c,dep}$ and station observations include anthropogenic input, but the $B_{c,dep}$ input to the
 229 SMB model is meant to reflect long-term non-anthropogenic sources of base cations. However, large point sources
 230 of $B_{c,dep}$ such as the AOSR are a feature of some Canadian regions, and their impact should not be overlooked in
 231 critical load assessments. Pollutant $B_{c,dep}$ from industrial sources can cause shifts in soil pH, plant community and
 232 biodiversity, as well as direct damage to vegetation by dust (e.g. Mandre et al., 2008; Paal et al., 2013). To
 233 demonstrate the relative impact of anthropogenic sources on Canadian critical loads estimates and to mitigate the
 234 impact anthropogenic local $B_{c,dep}$ inputs have in remote regions, two scenarios were assessed, one including
 235 anthropogenic $B_{c,dep}$ and another that attempted to smooth out anthropogenic “hot spots”. To demonstrate the relative
 236 impact of anthropogenic sources on Canadian critical loads estimates, two scenarios were assessed, one including
 237 anthropogenic $B_{c,dep}$ and another that attempted to smooth out anthropogenic “hot spots”.

238
 239 To reduce the influence of anthropogenic point sources, a smoothing filter was applied using the SAGA GIS module
 240 DTM Filter to identify local areas of locally intensified $B_{c,dep}$. Areas of $B_{c,dep}$ above a 30% increase relative to a 20-
 241 grid radius (approximately 50 km) were removed and infilled from their edges using inverse distance weighted
 242 interpolation. Note that forest fire emissions may be substantial and appear as $B_{c,dep}$ hot spots; for this application of
 243 the SMB, we have not added a forest fire term to the base cation budget because of the difficulty of accounting
 244 forest fire loss over the entire country. The loss of nitrogen due to forest fires from forest biomass and organic soil
 245 content is also significant (and not reflected in N_{ep} which only deals with loss from harvesting).

246 2.6 Soil runoff

247 Soil runoff was obtained from the hydrological model MetHyd (Bonten et al., 2016) following Reinds et al. (2015).
248 The data were resampled from the original resolution of $0.1 \times 0.05^\circ$ to 250 m and gaps were infilled from the edges.
249 A minimum Q was assigned ($10 \text{ m}^3 \text{ ha}^{-1} \text{ yr}^{-1}$) for broad regions where the coarse input soil map (FAO-UNESCO,
250 2003) used for hydrological modelling did not identify soil (i.e., exposed bedrock), but the high-resolution soil depth
251 and texture maps used for critical loads did identify soil.

252 2.7 Gibbsite equilibrium constant

253 The gibbsite equilibrium constant (K_{gibb}) describes the relationship between free (or unbound) aluminum
254 concentration and pH in the soil solution. As free aluminum concentrations are generally lower in the upper organic
255 horizons, observed ranges based on the organic matter content of the soil may be used to assign a K_{gibb} value. Soils
256 with organic matter less than 5% were assigned a value of $950 \text{ m}^6 \text{ eq}^{-2}$, soils with 5–15% organic matter were
257 assigned a lower value of $300 \text{ m}^6 \text{ eq}^{-2} \text{ yr}^{-1}$, and soils ranging from 15–30% organic matter were assigned a value of
258 $100 \text{ m}^6 \text{ eq}^{-2}$ (after CLRTAP, 2015).

259 2.8 Chemical criterion for damage

260 The critical base-cation-to-aluminum ratio (Bc/Al_{crit}) is the most widely used threshold, indicating damage to root
261 biomass. It is a simple approach that has been used in past Canadian estimates (e.g., Carou et al., 2008). In general,
262 it is applied as blanket or default value (e.g., $Bc/Al_{crit} = 1$) to a range of land cover types (e.g., forest or grassland).
263 In the current study, a species- and site-specific approach was used to assign damage thresholds for forest
264 ecosystems based on detailed tree species maps from the 2001 Canadian National Forest Inventory (NFI) (Beaudoin
265 et al., 2014). Two levels of protection were chosen to illustrate the difference between 20% acceptable growth
266 reduction (generally analogous to the default $Bc/Al_{crit} = 1$) versus a 5% growth reduction (generally analogous to
267 $Bc/Al_{crit} = 10$). Dose-response curves for Bc/Al_{crit} and root growth from Sverdrup and Warfvinge (1993) were
268 matched to species present in the NFI database (Table 2). If forest was present above 25% coverage, Values-values
269 were sorted by the most sensitive tree species (those with the lowest Bc/Al_{crit}) above 5% species composition and
270 given priority for the 250 m grid-cell value. If species-specific composition data for forests (from Beaudoin et al.,
271 2014) were not available, the Bc/Al_{crit} value was averaged to the genus; if no genus-level data were available, an
272 average coniferous, deciduous, or mixed forest value was applied. For non-forested soils, a default value based on a
273 representative species for the land cover type was used (e.g., 4.5 and 0.8 for 5% and 20% protection levels,
274 respectively, for grassland based on the response of *Deschampsia*).

277 **Table 2: Species-specific Bc/Al_{crit} values for 5% and 20% growth reduction scenarios following Sverdrup & Warfvinge**
278 **(1993). Genus-level or generalised land cover values were derived from representative species.**

Category	Bc/Al_{crit} (mol/mol)	
	5%	20%
Species (forest)		

Formatted: Normal

<i>Abies balsamea</i>	6.0	1.1
<i>Fagus grandifolia</i>	1.3	0.6
<i>Picea mariana</i>	2.5	0.8
<i>Pseudotsuga menziesii</i>	4.0	2.0
<i>Pinus strobus</i>	1.5	0.5
<i>Picea engelmannii</i>	2.5	0.5
<i>Pinus banksiana</i>	3.0	1.5
<i>Acer saccharum</i>	1.3	0.6
<i>Alnus glutinosa</i>	4.0	2.0
<i>Quercus rubra</i>	1.3	0.6
<i>Pinus ponderosa</i>	4.5	2.0
<i>Pinus resinosa</i>	4.5	2.0
<i>Picea rubens</i>	6.0	1.2
<i>Picea sitchensis</i>	2.5	0.4
<i>Larix laricina</i>	4.0	2.0
<i>Populus tremuloides</i>	8.0	4.0
<i>Tsuga heterophylla</i>	1.0	0.2
<i>Thuja plicata</i>	1.0	0.1
<i>Betula papyrifera</i>	4.0	2.0
<i>Picea glauca</i>	2.5	0.5
<i>Betula alleghaniensis</i>	4.0	2.0
<i>Betula populifolia</i>	4.0	2.0
<i>Picea abies</i>	6.0	1.2
<i>Pinus sylvestris</i>	3.0	1.2
Genus (forests)		
Abies	6.0	1.1
Acer	1.3	0.6
Alnus	4.0	2.0
Betula	4.0	2.0
Fagus	1.3	0.6
Larix	4.0	2.0
Picea	2.5	0.8
Pinus	3.0	1.5
Populus	8.0	4.0
Pseudotsuga	4.0	2.0
Quercus	1.3	0.6
Thuja	1.0	0.1
Tsuga	1.0	0.2
Generalised forest		
Deciduous	4.0	2.0
Coniferous	3.0	1.2
Mixed	3.0	1.2
Generalised land covers		
Grassland	4.5	0.8
Scrubland	2.8	0.6
Tundra	2.9	0.7

279

280 2.9 Base cation and nitrogen uptake

281 A species- and site-specific approach was also implemented to determine the net removal of nutrients (Ca, Mg, K,

282 N) through tree harvesting from forest ecosystems. Base cation uptake (BC_{up}) and N uptake (N_{up}) were estimated for

283 forest soils by assuming stem-only removal; site-specific stand bark and trunk biomass estimates (Beaudoin et al.,
 284 2014) were multiplied by average trunk- and bark-specific nutrient and base cation concentration data from the tree
 285 chemistry databases for each species present. Two ‘tree chemistry’ databases were merged to include as many tree
 286 species as possible (U.S. data: Pardo et al., 2005; Canadian data: Paré et al., 2013); duplicate studies were removed
 287 from the merged database and species data were averaged across studies. A simplifying assumption was made that
 288 stand biomass was related to the species composition (i.e., the dominant tree species in a stand is also the dominant
 289 contributor to biomass). The nutrient uptake maps were restricted to harvestable forest areas as delineated by
 290 Dymond et al. (2010) and in all other regions it were was set to 0. Nutrient uptake of other land types (e.g.,
 291 grasslands) was considered negligible since grazing takes place primarily in agricultural regions, which have been
 292 broadly masked out. Since B_{cup} cannot exceed inputs from deposition, weathering, and losses from leaching, a
 293 scaling factor was used to constrain base cation uptake between its maximum (that is, deposition + weathering –
 294 leaching) and a minimum calcium leaching value. The same scaling factor was applied to N_{up} .

295 2.10 Denitrification fraction

296 The soil denitrification fraction (f_{de}) is generally related to soil drainage (CLRTAP, 2015); classes ranging from
 297 excessive to very poor drainage were assigned using the Canada-wide Canadian Soil Information Service (CanSIS)
 298 databases v2.2 (CLBBR, 1996) and v.3.2 (SLCWG, 2010). Because the databases are not compatible in their
 299 geographic extent and alignment, boundary and classification priority was given to the most recent database version
 300 before rasterization. Differences in classifications and their alignment to the soil drainage classes from CLRTAP
 301 (2015) are shown in Table 3.~~The soil denitrification fraction (f_{de}) is generally related to soil drainage (CLRTAP,~~
 302 ~~2015); classes ranging from excessive to very poor drainage were assigned using the Canada-wide Canadian Soil~~
 303 ~~Information Service (CanSIS) databases v2.2 (CLBBR, 1996) and v.3.2 (SLCWG, 2010) (Table 3). In cases of~~
 304 ~~overlapping polygons from the two databases, boundary and classification priority was given to the most recent~~
 305 ~~database version before rasterization.~~

306
 307 **Table 3: Denitrification fraction (f_{de}) values (adapted from CLRTAP, 2015) and their corresponding drainage**
 308 **classifications in versions 2.2 and 3.2 of the Canadian Soil Information Service database.**

Drainage	f_{de}	V2.2	V3.2
Excessive	0	E/R	VR/R
Good	0.1	W	W
Moderate	0.2	M	MW
Imperfect	0.4	I	I
Poor	0.7	P	P
Very poor	0.8	V	VP

309

310 2.11 Deposition and exceedance

311 Exceedances for both acidity and nutrient nitrogen were calculated ~~against-using~~ total deposition maps of annual
312 total S and N, which were sourced from GEM-MACH model output at 10 km horizontal grid spacing (GEM-MACH
313 v3.1.1.0, RAQDPS version 023) (Moran et al., 2024a, b). A three-year (2014–2016) annual average was taken to
314 reduce inter-annual variability in deposition, where input emissions based on annual emissions inventories specific
315 to each of these three years were used for the three annual runs. Note that Moran et al. (2024b) have presented
316 detailed evaluations of some components of these deposition estimates, specifically ambient concentration (as a
317 proxy for dry deposition) and wet deposition of SO₂ and particle sulphate (p-SO₄), HNO₃ and p-NO₃, and NH₃ and
318 p-NH₄, that suggest that they are robust.

319
320 Exceedances of critical load for both acidity and nutrient nitrogen (on a 250 m grid) were summarized to the 10 km
321 deposition grid using Average Accumulated Exceedance (AAE), which is an area-weighted average that considers
322 ecosystem coverage within each grid cell to derive the average of the summed exceedance; this addresses issues
323 with sparse coverage and considers all ecosystems within the grid (Posch et al., 1999). The [Canadian Protected and](#)
324 [Conserved Areas Database \(CPCAD\)](#) was used to identify areas in exceedance that may be of particular concern to
325 policymakers— (ECCC, 2023b). The database, assembled in support of Canada’s reporting on Canadian
326 Environmental Sustainability Indicators and the UN Convention on Biological Diversity (among other initiatives),
327 identifies Protected Areas (PA) such as national and provincial parks as well as Other Effective area-based
328 Conservation Measures (OECM). Interim areas were included in expectation of their formal establishment. Areas
329 that fell entirely within the agricultural ecumene were removed, but areas that straddled the ecumene were retained.
330 Areas were counted as in exceedance if any part of the area experienced exceedance at the 250 m resolution.

331
332 The exceedance calculations used for acidity employed the methodology described by Posch et al. (2015), where the
333 critical load function (Figure 2) was divided into five regions, and a different formula for exceedance was used for
334 each region. Five inputs for each 250 m grid cell were required for these calculations: the S and N total deposition
335 pair plus CL_{maxS} , CL_{minN} , and CL_{maxN} values. For S and N total deposition pairs falling into four of the regions, the
336 exceedance value will be positive (i.e., in exceedance) and its magnitude indicates how great the S and N acidic
337 deposition at the location is above the critical load for acidity. For the Region 0, the exceedance value will be
338 negative (i.e., not in exceedance) and its magnitude will give how far the S and N acidic deposition is below the
339 critical load for acidity. Calculation of nutrient N exceedance was simply the difference between N_{dep} and CL_{nutN} .

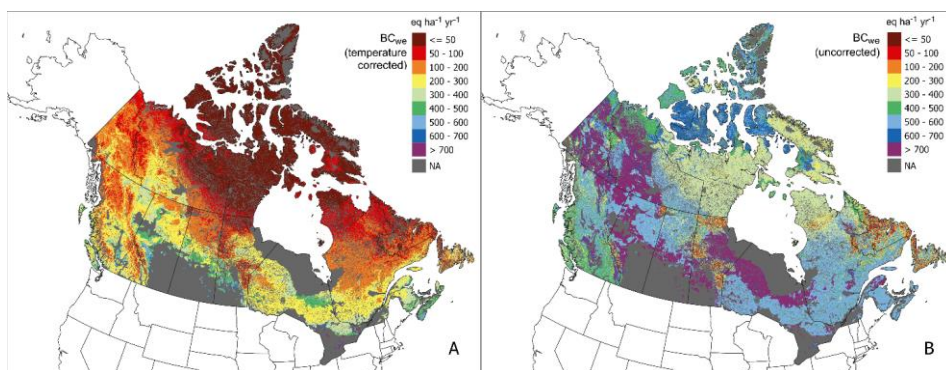
340 3 Results

341 3.1 Base cation weathering

342 The estimated BC_{we} was very low (below 100 eq ha⁻¹ yr⁻¹) for nearly all regions north of 60°N latitude, and low
343 (below 200 eq ha⁻¹ yr⁻¹) for many northern regions south of 60°N latitude (Figure 4A). Higher BC_{we} (above 500 eq
344 ha⁻¹ yr⁻¹) was predicted for the calcareous and deep soils of the Prairies and southern Ontario adjacent to agricultural

345 regions (i.e. the mean Prairie average for natural and semi-natural soils was 714 eq ha⁻¹ yr⁻¹), although most of these
 346 ecozones are excluded as part of the agricultural ecumene (Table 4). Average BC_{we} for the Arctic ecozones was <
 347 50 eq ha⁻¹ yr⁻¹, in contrast with $BC_{we} > 700$ for Mixed Wood Plain and Prairie ecozones. Similarly, provincial
 348 averages were lowest for Nunavut and highest for Saskatchewan (Table 4). Base cation weathering without
 349 temperature correction (Figure 4B, mean value of 570 eq ha⁻¹ yr⁻¹) illustrates the strong effect temperature has on
 350 limiting BC_{we} in most of the country (average 173 eq ha⁻¹ yr⁻¹), particularly Arctic and mountainous regions.

351



352

353 **Figure 4:** Base cation weathering rate (Ca+Mg+K+Na) with temperature correction (A) and without (B). The weathering
 354 rate was estimated using a soil texture approximation method with sand, clay, and parent material acid class modified by
 355 depth (see Section 2.4).

356 **Table 4:** Ecozone and provincial mean values for inputs and outputs of the Simple Mass Balance model, including base
 357 cation weathering (BC_{we}), smoothed base cation deposition (BC_{dep}), base cation uptake (BC_{up}), nitrogen uptake (N_{up}),
 358 critical base-cation-to-aluminum ratio (Bc/Al_{crit}) for under 5% and 20% growth reductions-scenarios, average sulphur
 359 deposition ($DepS$) and nitrogen deposition ($DepN$) 2014 - 2017, maximum critical load of sulphur (CL_{maxS}), maximum
 360 critical load of nitrogen (CL_{maxN}), minimum nitrogen critical load (CL_{minN}) and critical load of nutrient nitrogen (CL_{nutN}).
 361 Units are in eq ha⁻¹ yr⁻¹ except for Bc/Al_{crit} which is a unitless ratio. The critical loads presented in the table were
 362 calculated using the 5% Bc/Al_{crit} and the smoothed BC_{dep} . Note that values represent coverage-averages over eligible soils
 363 (e.g. excluding agricultural areas and organic soils).

Ecozone	BC_{we}	BC_{dep}	BC_{up}	N_{up}	Bc/Al_{crit} 5%	Bc/Al_{crit} 20%	$DepS$	$DepN$	CL_{max} S	CL_{max} N	CL_{min} N	CL_{nut} N
Arctic Cordillera	40	5	< 1	< 1	5.2	1.2	8	21	82	88	36	173
Atlantic Maritime	353	89	32	37	5.7	1.1	57	240	615	551	36	234
Boreal Cordillera	174	19	5	5	3.9	1.2	10	29	290	274	36	77
Boreal Plain	331	139	27	23	3.7	1.4	38	172	802	549	36	71
Boreal Shield	229	84	18	23	4.0	0.9	53	206	512	422	36	147
Hudson Plain	212	56	< 1	< 1	2.8	0.8	30	111	499	221	36	104
Mixedwood Plain	712	180	< 1	< 1	3.6	0.9	137	712	1586	1171	36	145
Montane Cordillera	240	52	39	42	3.6	1.2	25	98	447	473	40	164
Northern	32	7	< 1	< 1	5.6	1.3	9	20	63	75	41	75

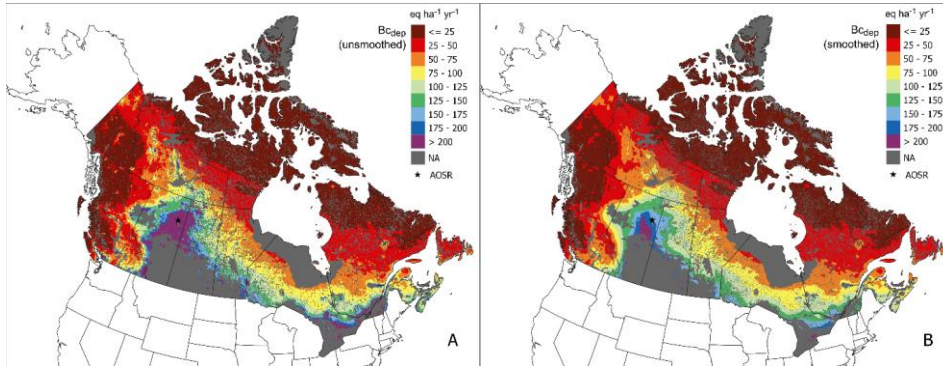
Arctic													
Pacific	274	25	78	135	2.9	0.9	53	172	608	1281	48	513	
Maritime													
Prairie	559	191	13	2	5.0	1.9	54	423	1078	893	59	63	
Southern	45	21	< 1	< 1	5.6	1.3	10	26	112	118	60	65	
Arctic													
Taiga	106	31	< 1	< 1	4.3	1.0	10	26	218	194	76	66	
Cordillera													
Taiga Plain	195	51	4	4	3.2	1.0	13	37	390	246	79	51	
Taiga	88	40	< 1	< 1	3.5	0.8	18	54	227	200	192	110	
Shield													
Province													
Alberta	285	133	24	17	3.7	1.4	35	142	730	512	58	78	
British	235	37	40	53	3.6	1.2	26	92	439	551	91	206	
Columbia													
Manitoba	217	86	7	7	2.9	0.9	41	146	512	338	44	66	
New	344	91	34	41	5.8	1.1	49	227	595	502	79	243	
Brunswick													
Newfoundl	110	24	6	7	4.6	0.9	24	71	217	190	43	223	
and &													
Labrador													
Nova Scotia	422	92	21	28	5.6	1.1	68	249	733	652	65	261	
Northwest	114	41	< 1	< 1	4.0	1.0	11	28	254	191	36	49	
Territories													
Nunavut	34	11	< 1	< 1	5.5	1.2	9	22	75	87	36	75	
Ontario	306	103	23	19	3.8	0.9	61	289	666	509	66	141	
Prince	422	69	19	18	5.3	1.0	57	209	672	558	66	226	
Edward													
Island													
Québec	148	46	11	14	4.5	1.0	38	132	314	299	50	153	
Saskatchewan	230	124	12	8	3.1	1.0	29	128	607	492	49	62	
an													
Yukon	148	25	< 1	< 1	3.8	1.0	10	26	266	233	36	54	
Canada	132	52	8.2	10	4.5	1.1	76	22	291	258	48	99	

364

365 3.2 Base cation deposition

366 Modelled BC_{dep} ranged from low ($< 25 \text{ eq ha}^{-1} \text{ yr}^{-1}$) in the north to higher values ($> 200 \text{ eq ha}^{-1} \text{ yr}^{-1}$) around the
367 Prairies and the southern regions of the eastern provinces (Figure 5) as well as in Alberta and Saskatchewan (Table
368 4). Average (smoothed) BC_{dep} was roughly one-third of BC_{we} . Hot spots of $BC_{dep} - BC_{dep}$ associated with at
369 anthropogenic point sources (e.g., from mining operations as well as the contribution from the AOSR) were clearly
370 visible in the unsmoothed map (Figure 5A). The smoothing algorithm (Figure 5B) eliminated most of the effects of
371 point sources, at the cost of ~~some loss of definition~~ lowering average BC_{dep} (Canada-wide average of ~~52-68~~ $52-68 \text{ eq ha}^{-1} \text{ yr}^{-1}$
372 ~~pre-smoothing and 68-52~~ $68-52 \text{ eq ha}^{-1} \text{ yr}^{-1}$ post-smoothing). However, it did not completely erase elevated BC_{dep} in the
373 AOSR; the difference in size between other point source footprints and the AOSR necessitated a compromise in

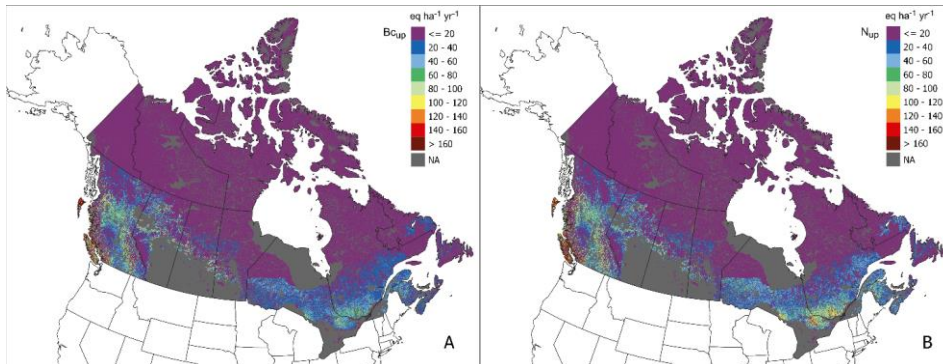
374 filter radius and slope selection. The smoothed BC_{dep} was adopted as the primary data set for presenting the critical
 375 loads.



376
 377 **Figure 5: Non-sea-salt base cation deposition (Ca + Mg + K) with anthropogenic contributions (A) and after a smoothing**
 378 **filter was applied to reduce the effect of anthropogenic point sources (B).** The location of the city of Fort McMurray
 379 within The Athabasca Oil Sands Region (AOSR) is identified by a star.

380 3.3 Base cation and nitrogen uptake

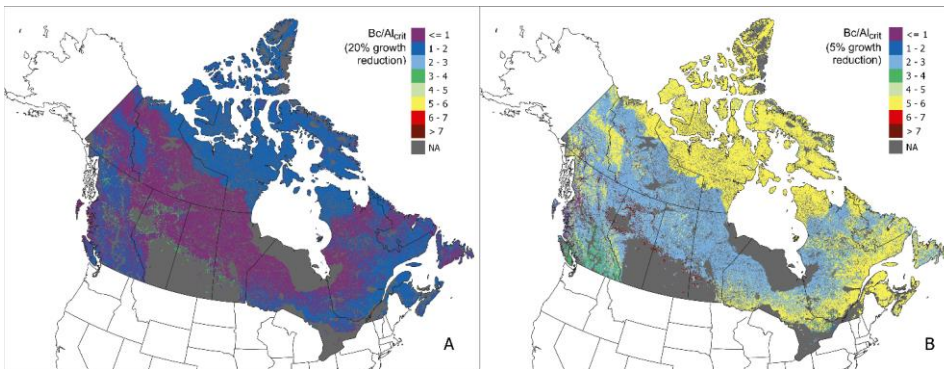
381 Base cation uptake ranged from < 1 to $545 \text{ eq ha}^{-1} \text{ yr}^{-1}$ and was highest in coastal British Columbia; the Pacific
 382 Maritime ecozone had the highest mean BC_{up} at $79 \text{ eq ha}^{-1} \text{ yr}^{-1}$ (Table 4). Nitrogen uptake was also high in British
 383 Columbia and the Pacific Maritime zone (mean N_{up} of $135 \text{ eq ha}^{-1} \text{ yr}^{-1}$) as well as the Montane Cordillera (mean N_{up}
 384 of $42 \text{ eq ha}^{-1} \text{ yr}^{-1}$). Regions of elevated N_{up} were seen in eastern Ontario and southern Quebec (Figure 6); these occur
 385 on the Boreal Shield ecozone, which is a large ecozone that extends across multiple provinces over which N_{up} varies
 386 (but with a mean value of $23 \text{ eq ha}^{-1} \text{ yr}^{-1}$).



387
 388 **Figure 6: Base cation (Ca+Mg+K) uptake (A) and nitrogen uptake (B): forested regions limited to harvestable regions**
 389 **(identified by Dymond et al. (2010)). Uptake for non-forested ecosystems was set to 0.**

390 **3.4 Critical base-cation-to-aluminum ratio**

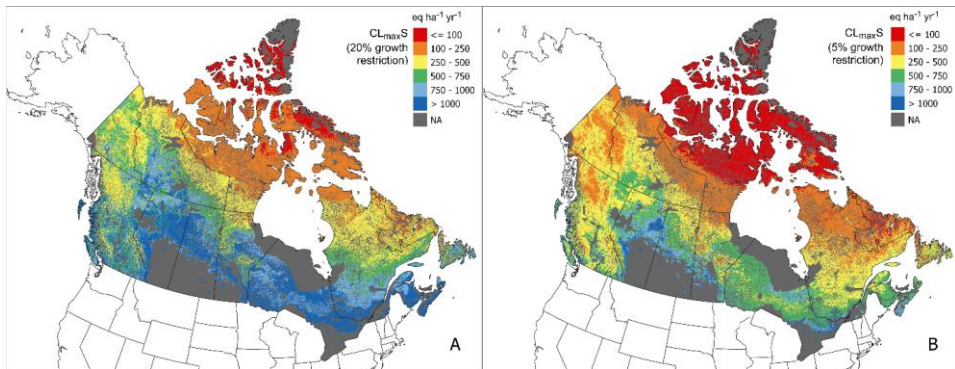
391 Almost the entire country fell below a Bc/Al_{crit} ratio of 2 under 20% root biomass growth reduction (Figure 7A). In
392 contrast, a Bc/Al_{crit} ranged from 1–8 (average = 4.4) under the 5% root biomass growth reduction (Figure 7B). The
393 ratio ranged from 3–6 for forests in eastern Canada (A and B ecozones), while ranges for the Boreal Shield ecozone
394 were 2–4 and coastal forest in British Columbia were slightly higher at 3–4. Semi-natural grassland in the Prairies
395 were given a ratio of 4.5 based on *Deschampsia*, but many fringe regions of the Prairies are treed and dominated by
396 *Populus tremuloides*, which had a Bc/Al_{crit} of 8.



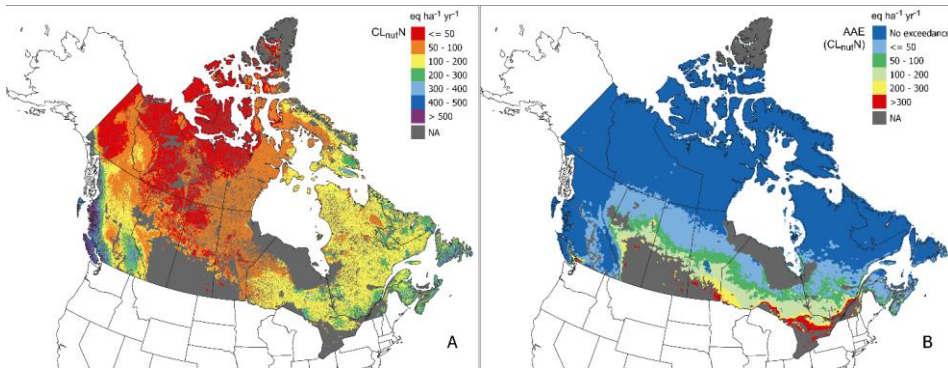
397
398 **Figure 7: Critical base-cation-to-aluminum ratio (Bc/Al_{crit}) under a 20% growth reduction (A) and a 5% growth**
399 **reduction (B). Site-specific ratios were selected for each 250 m grid cell for the most sensitive species (or genus or land-**
400 **cover type if no species data available). Note that while the legends have been matched for comparison, the maximum**
401 **ratio in the 20% growth reduction map is 4.**

402 **3.5 Critical loads**

403 The CL_{maxS} under the 20% protection level (i.e., allowing more damage) showed low sensitivity ($> 1000 \text{ eq ha}^{-1} \text{ yr}^{-1}$)
404 to acidic deposition for most regions below 55°N latitude (Figure 8A). In contrast, under the 5% protection level
405 (Figure 8B), low sensitivity was limited to southern agricultural regions in the Prairies. Lowest CL_{maxS} and CL_{maxN}
406 were found in the Arctic territories (Nunavut, the Northwest Territories, the Yukon; Table 4) and also
407 Newfoundland and Labrador (Figure 12B). Of the provinces, Quebec had the lowest CL_{maxS} ($314 \text{ eq ha}^{-1} \text{ yr}^{-1}$) and
408 CL_{maxN} ($299 \text{ eq ha}^{-1} \text{ yr}^{-1}$) (Table 4). From an ecozone perspective the Mixedwood Plain ecozone had the highest
409 CL_{maxS} at $1586 \text{ eq ha}^{-1} \text{ yr}^{-1}$ followed by the Prairies at $1078 \text{ eq ha}^{-1} \text{ yr}^{-1}$. The most sensitive ecozones outside the
410 Arctic ecozones (which were below $100 \text{ eq ha}^{-1} \text{ yr}^{-1}$) were the Boreal Cordillera and the Taiga ecozones (Table 4).
411 For CL_{minN} , central and northern regions of the country were sensitive to nutrient N deposition, particularly pastures,
412 grasslands, scrublands, and sparse forest in and surrounding the Prairies (Figure 9A). Further, very low CL_{minN} (\leq
413 $75 \text{ eq ha}^{-1} \text{ yr}^{-1}$ were estimated over the Arctic territories (Table 4) as well as in northern Alberta and the Athabasca
414 Basin in northern Saskatchewan. The coastal ecozones had the highest CL_{minN} , with the Pacific and Atlantic
415 Maritime zones having 513 and $235 \text{ eq ha}^{-1} \text{ yr}^{-1}$ respectively. The Prairie ecozone had the lowest CL_{minN} , lower than
416 some of the Arctic ecozones, at $63 \text{ eq ha}^{-1} \text{ yr}^{-1}$.



418
419 **Figure 8: Maximum sulphur critical load (CL_{maxS}) at a 20% growth restriction scenario (A) versus a 5% growth**
420 **restriction scenario (B), using reduced-anthropogenic (i.e., smoothed) Bc_{dep} .**



421
422 **Figure 9: Critical load of nutrient nitrogen using the SMB model (A) and average accumulated exceedance of nutrient**
423 **nitrogen (B) estimated under modelled total deposition of nitrogen from 2014–2016.**

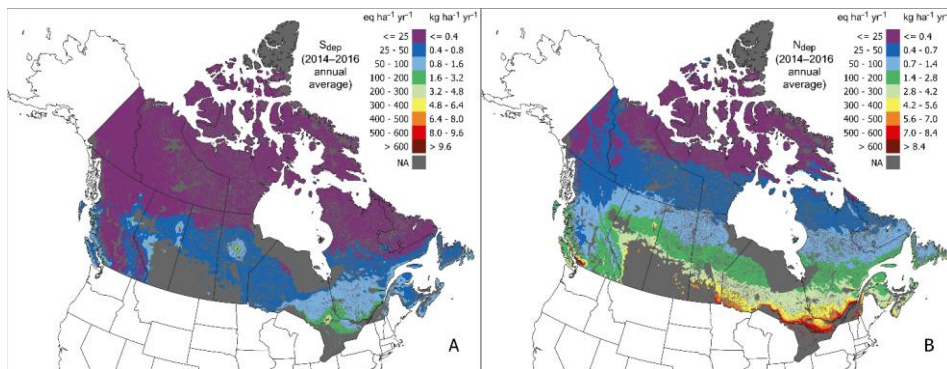
424

425 3.6 Deposition

426 Modelled average annual S_{dep} was below 25 eq ha⁻¹ yr⁻¹ for most of the country above 59°N, as well as the Montaine
427 Cordillera ecozone that covers much of British Columbia (Figure 9A10A). Southern Quebec and central Ontario
428 showed higher annual average values between 50–200 eq ha⁻¹ yr⁻¹, with some point sources showing S_{dep} in excess
429 of 500 eq ha⁻¹ yr⁻¹ (e.g., at nickel smelters and mining operations in Sudbury, Ontario and Thompson,
430 Manitoba). Southern Quebec and central Ontario showed higher annual average values between 50–200 eq ha⁻¹ yr⁻¹,
431 with some isolated point sources showing S_{dep} in excess of 500 eq ha⁻¹ yr⁻¹. Modelled average annual N_{dep} (Figure
432 9B) exceeded S_{dep} in most parts of the country. A north-south N_{dep} gradient is observable in Figure 10B, showing
433 higher N_{dep} closer to agricultural sources in southern Ontario and Quebec and in the Prairies. Nitrogen deposition

Formatted: Normal

434 exceeding 500 eq ha⁻¹ yr⁻¹ was present in northern Ontario and southern Quebec as well as southern Manitoba and
435 southwestern British Columbia.



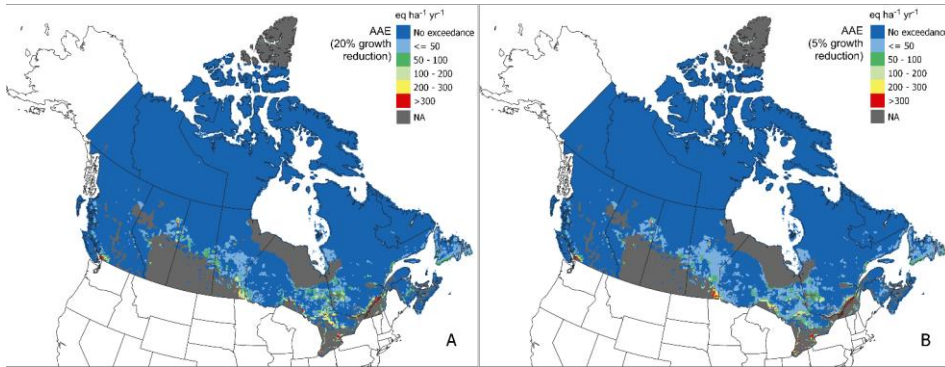
436
437 **Figure 109: Modelled total deposition annual average (2014–2016) total deposition of sulphur (S_{dep} , panel A) and nitrogen**
438 **(N_{dep} , panel B) under average annual deposition from 2014–2016. Maps were sourced from GEM-MACH (Moran et al.,**
439 **2024a, b).**

440 3.7 Exceedances

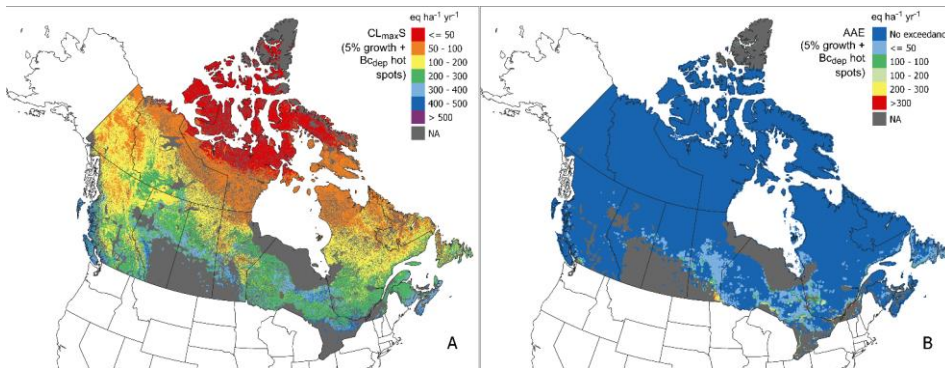
441 Widespread but low exceedances of acidity (< 50 eq ha⁻¹ yr⁻¹) under average 2014–2016 deposition were found in
442 regions in central and southern Quebec, Ontario, Manitoba, Alberta, British Columbia as well as in some regions in
443 Nova Scotia and Newfoundland, under both protection levels (Figure 1011). Further, exceedances above 200 eq ha⁻¹
444 yr⁻¹ were predicted in southern Quebec and Ontario, as well as near Winnipeg and Vancouver, under both protection
445 levels. Exceedances of acidity under 2014–2016 S and N deposition were not generally predicted in the north. The
446 spatial extent of exceedance was slightly greater under the 5% protection limit as a result of higher/lower $CL_{max}S$ and
447 $CL_{max}N$, particularly around point sources of S and N, such as the AOSR.

448
449 If the B_{cdep} without smoothing is employed (i.e., the base cation deposition associated with high magnitude
450 anthropogenic sources is included), exceedances are reduced (see Figure 1112(B) and compare to Figure 1011(B)).
451 The $CL_{max}S$ based on anthropogenic-inclusive B_{cdep} (at 5% protection level, Figure 11A12A) indicated that $CL_{max}S$ is
452 elevated in the AOSR in comparison with the smoothed $CL_{max}S$ in Figure 8B.

453



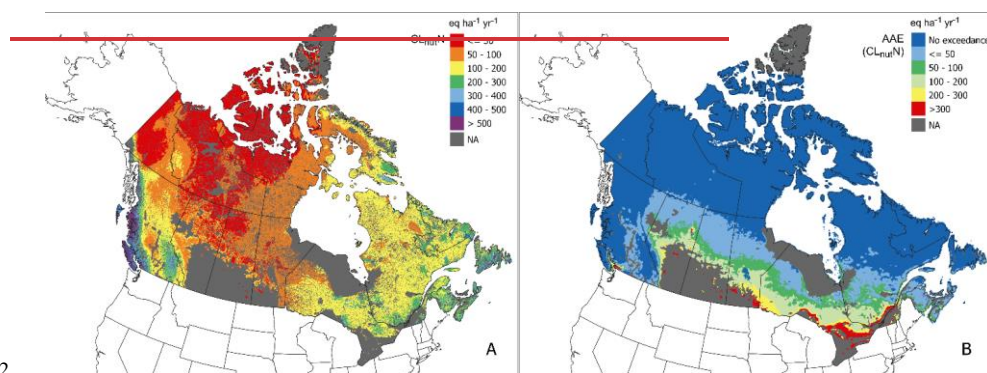
454
 455 **Figure 1011:** Average Accumulated Exceedance (AAE) of critical loads of acidity under 2014–2016 sulphur plus and
 456 nitrogen GEM-MACH modelled deposition. Two growth reduction scenarios are presented: using a chemical criterion
 457 representing 20% growth reduction (A) and 5% growth reduction (B).



458
 459 **Figure 1412:** A scenario including using base cation deposition without smoothing, illustrating the impact of hot-spot
 460 B_{Cdep} on the maximum critical load of sulphur (CL_{maxS}) (A) and the Average Accumulated Exceedance (AAE) under
 461 average 2014–2016 sulphur plus and nitrogen GEM-MACH modelled deposition (B).

462 For CL_{minN} , central and northern regions of the country were sensitive to nutrient N deposition, particularly pastures,
 463 grasslands, scrublands, and sparse forest in and surrounding the Prairies (Figure 12A). Further, very low CL_{minN} (\leq
 464 $75 \text{ eq ha}^{-1} \text{ yr}^{-1}$) were estimated over the Arctic territories (Table 4) as well as in northern Alberta and the Athabasca
 465 Basin in northern Saskatchewan (Figure 12A). Widespread exceedances of CL_{minN} were predicted across most
 466 provinces, with generally low AAE ($< 50 \text{ eq ha}^{-1} \text{ yr}^{-1}$) extending to just north of 60° latitude, and higher values of
 467 $100\text{--}200 \text{ eq ha}^{-1} \text{ yr}^{-1}$ were predicted from Alberta east to Quebec (Figure 12B9B). Some regions adjacent to the
 468 agricultural ecumene in the Prairies, southern Ontario, Quebec and the AOSR experienced values above 300 eq ha^{-1}
 469 yr^{-1} up to $1053 \text{ eq ha}^{-1} \text{ yr}^{-1}$; however, 80% of grid cells in exceedance fell below $300 \text{ eq ha}^{-1} \text{ yr}^{-1}$. Some regions
 470 adjacent to the agricultural ecumene in the Prairies, southern Ontario, Quebec and the AOSR experienced values
 471 above $300 \text{ eq ha}^{-1} \text{ yr}^{-1}$ (Figure 12B).

473
 474 There were 12,341 sites of interest across Canada (i.e., PA and OECM areas); however, only 8,372 fall within areas
 475 assessed in this study (e.g. not within the agricultural ecumene or Hudson Bay Plains ecozone). In total, 10% of
 476 these sites exceeded CL_{maxS} under the 5% protection limit (Table 5). This was roughly double the number of sites in
 477 exceedance under the 20% protection limit. By comparison the $B_{C_{dep}}$ layer with unsmoothed hot spots (i.e. retaining
 478 higher $B_{C_{dep}}$ close to anthropogenic emissions areas) under the 5% protection limit showed a reduction in total areas
 479 that are in exceedance of acidity critical loads; anthropogenic emissions of base cations reduce the exceedances by
 480 ~~reducing~~ increasing N_{up} values. The number of PA and OECM sites in exceedance of CL_{nutN} was much higher, 70%
 481 of total sites assessed (Table 5).



482
 483 **Figure 12: Critical load of nutrient nitrogen using the SMB model (A) and average accumulated exceedance of nutrient**
 484 **nitrogen (B) estimated under modelled total deposition of nitrogen from 2014–2016.**

Formatted: Caption

485
 486 **Table 5: Exceedance summarized by number of Protected Areas (PA) and Other Effective area-based Conservation**
 487 **Measures (OECM) areas (ECCC, 2023b) experiencing any exceedance. Three exceedance scenarios are presented:**
 488 **Critical load of acidity exceedance at 5% and 20% growth reduction protection levels, unsmoothed base cation deposition**
 489 **under the 5% scenario, and exceedance of nutrient nitrogen (CL_{nutN}). Critical loads of acidity and nutrient nitrogen were**
 490 **assessed under a multi-year (2014–2016) average GEM-MACH modelled sulphur and nitrogen total deposition.**

	PA	OECM	% Exceeded
Number of sites	8,205	167	-
Exceeded (5% growth reduction)	793	17	9.7
Exceeded (20% growth reduction)	313	10	3.9
Exceeded (5% with hot spots)	445	14	5.5
Exceeded (CL_{nutN})	5,807	85	70.4

491

492 4 Discussion

493 4.1 Uncertainties ~~in~~ critical loads of acidity and nutrient nitrogen

494 Critical loads of acidity reflect the influence of BC_{we} , particularly in the north where cold annual temperatures slow
495 weathering rates to almost zero. However, areas near the Canada-U.S. border also showed lower BC_{we} rates by 200–
496 300 eq ha⁻¹ yr⁻¹ when corrected for temperature (Figure 4). Soil depth remains a poorly mapped parameter that has
497 significant impact on BC_{we} , and it is worth noting that average estimates were based on mapped soil depths (Hengl,
498 2017), which ranged from 1 cm to a maximum rooting depth of 30 or 50 cm. While comparison between mapped
499 values and site-level values is difficult (due to methodological differences and spatial representation), there are some
500 studies which have observational values in representative areas; for example, in northern Saskatchewan, 50% of 107
501 sites were estimated below 300 eq ha⁻¹ yr⁻¹, slightly above our mapped estimates of 230 eq ha⁻¹ yr⁻¹ for (primarily
502 northern) Saskatchewan (Table 4; Figure 4). Estimates for conifer stands in Québec by Ouimet et al. (2001) were
503 210 eq ha⁻¹ yr⁻¹, comparable to the mean 229 eq ha⁻¹ yr⁻¹ estimated for the Boreal Shield ecozone in our study (Table
504 4). In British Columbia, Mongeon et al. (2010) found BC_{we} to be 710 eq ha⁻¹ yr⁻¹, much greater than the 235 eq ha⁻¹
505 yr⁻¹ estimated in our study for the Pacific Maritime ecozone. Koseva et al., (2010) estimated BC_{we} at 10 sites in
506 Ontario primarily in the Mixedwood Plains ecozone at 628 eq ha⁻¹ yr⁻¹ (compared to 306 eq ha⁻¹ yr⁻¹ over the
507 Mixedwood Plains in our study). Moreover, Koseva et al. suggest that the soil-texture approximation method (as
508 used in our study) under-estimates BC_{we} in comparison to the better-performing PROFILE model. Assessments of
509 uncertainty in critical load estimates recognize BC_{we} as the primary driver of uncertainty (Li and ~~MenuliyMcNulty~~,
510 2007; Skeffington et al., 2006) and, as such, observational data and PROFILE-modelled site data to constrain
511 weathering rates would greatly improve critical load estimates.

512
513 While the inclusion of a modelled BC_{dep} map represents an improvement over previous Canadian critical load ~~map~~
514 projects, several factors likely contribute to the BC_{dep} modelled negative bias (which has appeared in other
515 publications, such as Makar et al., 2018), ~~and~~ ~~and~~ may relate to how emissions processing has been carried out for
516 air-quality models in North America. While anthropogenic emissions inventories include estimates of PM_{2.5}, PM₁₀
517 and PM_{total} mass emissions, usually only PM_{2.5} and PM₁₀ emissions are used in determination of model input
518 emissions. However, substantial emitted base cation mass may reside in the larger size fractions (between the mass
519 included within PM₁₀ and the PM_{total}). The model version and emissions inventory data used in the base cation
520 deposition estimates of AQMEII4 included only emissions up to 10 µm diameter, as did work examining emissions
521 from multiple sources of primary particulate matter (Boutzis et al., 2020). Subsequent work using observations from
522 the Canadian Oil Sands and reviewing other sources of data ~~subsequent to~~ ~~after~~ Boutzis et al. (2020) and Galmarini
523 et al. (2021) suggest that many of the same sources of anthropogenic particulate matter emissions include emitted
524 particles between 10 and 40 µm diameter, the mass of which adds an additional 66% relative to the PM_{2.5} to PM₁₀
525 “coarse mode” emitted mass. For forest fire emissions, this additional mass is much larger. The wildfire particulate
526 matter size distributions of Radke et al. (1988; 1990) used to estimate mass up to PM₁₀ in Boutzis et al. (2020) show
527 that the emitted particle mass between 10 and 40 µm diameter is 7.26 ~~times~~ that emitted between PM_{2.5} and PM₁₀.
528 Approximately 9.7% of this particle mass is composed of base cations (e.g., Table S5 of Chen et al., 2019). A third

529 factor is another natural emissions source, aeolian or wind-blown dust emissions (e.g., Bullard et al., 2016; Park et
530 al., 2010), which was not included in the AQMEII4 simulations. These (traditionally missing) sources of base
531 cation mass in air-quality models likely contribute to the substantial negative bias noted here. Nevertheless,
532 regression in Figure 3 suggests that the spatial distribution of base cations emissions and deposition from Galmarini
533 et al. (2021) is reasonable, and we have used the relationship between modelled and observed values to provide
534 corrected estimates of Bc_{dep} .

535
536 The conservative 5% protection level set for the Bc/Al_{crit} is favoured by the authors of the current work for critical
537 loads estimates, which affords greater ecosystem protection consistent with studies using $Bc/Al > 1$ (e.g. McDonnell
538 et al., 2023; Mongeon et al., 2010; Ouimet et al., 2006). Historically, when acidic deposition was higher than at
539 present, a 20% growth reduction was a reasonable target. However, under decreasing emissions and deposition, as
540 well as acceptable impacts to wood production, carbon storage, and ecosystem health there is greater certainty in
541 ecosystem protection under the 5% protection level. It should be noted that the level of protection is a policy
542 decision regarding how much should be protected, rather than a sensitivity.~~It should be noted that the level of~~
543 ~~protection is an ethical choice regarding how much should be protected, rather than a sensitivity,~~ and taking the most
544 sensitive species through the Bc/Al_{crit} selection process ensures the highest possible protection based on species-
545 specific dose-response curves. Note, however, that changes to forest health and climate may also induce pressures
546 that are not captured in the selection of the Bc/Al_{crit} from the studies described in Sverdrup & Warfvinge (1993).

547
548 $CL_{min}N$ seems to be driven primarily by Q rather than by vegetation cover; low $CL_{min}N$ was seen in regions of
549 correspondingly low Q values (e.g., $>50 \text{ mm yr}^{-1}$) in much of the Arctic and central Canada. In contrast, areas with
550 high Q were found to result in high $CL_{min}N$; as previously suggested by Reinds et al. (2015), a critical flux rather
551 than concentration may provide more reliable critical loads in regions with elevated precipitation such as the Pacific
552 Maritime ecozone in British Columbia.

553 ~~Low $CL_{min}N$ in the Arctic was driven by very low Q values on thin barren land covers. In contrast, areas with high Q~~
554 ~~were found to result in high $CL_{min}N$; as previously suggested by Reinds et al. (2015), a critical flux rather than~~
555 ~~concentration may provide more reliable critical loads in regions with elevated precipitation such as the Pacific~~
556 ~~Maritime ecozone in British Columbia.~~

557
558 The omission of wetlands, which cover an estimated 13% of land in Canada, from acidity and nutrient N critical
559 loads represents a gap in terrestrial (and aquatic) ecosystem protection. Although there are modifications to the
560 SMB model that address critical loads for wetlands, this study was limited by the availability of a suitable national
561 wetlands classification map. Future studies may address this data gap as wetland classification products become
562 available.

563 4.2 Exceedances of critical loads

564 Historically, forests in eastern Canada were regarded as ~~the region ecosystems~~ most susceptible to acidification due
565 to their underlying geology, shallow soil type, vegetation, and elevated acidic deposition from domestic and
566 transboundary air pollution. This study adds to the body of literature supporting recent studies in both terrestrial and
567 aquatic critical loads (e.g., Makar et al., 2018; Cathcart et al., 2016; Williston et al., 2016; Mongeon et al., 2010;
568 Whitfield et al., 2010), showing likely exceedance of critical loads of acidity in central and western Canada (i.e., in
569 regions such as Alberta, Saskatchewan and British Columbia). The prevalence of our predicted widespread
570 exceedances in Manitoba (Figure 10) may reflect low mineral soil depth, as organic soil dominates this part of the
571 country. Further, point sources (generally large mining or smelting operations) remain a concern (e.g., in southern
572 Manitoba, the AOSR, and southern British Columbia) with regard to sharply elevated local exceedance, which may
573 be temporally mitigated by elevated BC_{dep} from co-located dust emissions sources. Additionally, high BC_{dep} can have
574 an alkalinizing impact on ecosystems. In China, where elevated BC_{dep} emissions from industrialization have
575 historically mitigated the effects of acidic deposition in many regions, successful particle emissions mitigation
576 strategies have reduced BC_{dep} in recent years (as S and N deposition have declined), resulting in increased critical
577 load exceedance (Zhao et al., 2021). However, the steady-state assumptions of the SMB require non-anthropogenic
578 BC_{dep} , since they must reflect long-term conditions, and base cation emissions cannot be reliably coupled with
579 changes to those of S and N and should be considered separately.

580
581 Widespread $CL_{nut}N$ exceedance (found in the majority of the PA and OECM sites assessed) suggests that nutrient N
582 may present a risk to biodiversity at many sites under protective measures. However, 40% of the grid cells showing
583 $CL_{nut}N$ exceedance were below $50 \text{ eq ha}^{-1} \text{ yr}^{-1}$ and it is likely that many of these exceedances are within the
584 uncertainty of the model. While some empirical studies of nutrient N have been done in Canada, a large knowledge
585 gap exists for many Canadian ecosystems regarding the effect of nutrient nitrogen and their critical loads. Some
586 work has developed on Jack pine and northern ecosystems; Vandinthner suggested that across Jack pine-dominant
587 forests surrounding the AOSR, the biodiversity-based empirical critical load of nutrient N was $5.6 \text{ kg ha}^{-1} \text{ yr}^{-1}$ (400
588 $\text{eq ha}^{-1} \text{ yr}^{-1}$; Vandinthner and Aherne, 2023a) which is above the maximum $CL_{nut}N$ calculated in this study within 200
589 km of the AOSR ($216 \text{ eq ha}^{-1} \text{ yr}^{-1}$). Further, in low deposition ‘background’ regions a biodiversity-based empirical
590 critical load of $1.4 - 3.15 \text{ kg ha}^{-1} \text{ yr}^{-1}$ ($100 - 225 \text{ eq ha}^{-1} \text{ yr}^{-1}$) was found to protect lichen communities and other N-
591 sensitive species in Jack pine forests across Northwestern Canada (Vandinthner and Aherne, 2023b); these are again
592 higher compared to mean values in this study (e.g. for the Boreal Plain, $76 \text{ eq ha}^{-1} \text{ yr}^{-1}$). Empirical critical loads
593 developed for ecoregions in Northern Saskatchewan (Murray et al., 2017) fall into a range of $88 - 123 \text{ eq ha}^{-1} \text{ yr}^{-1}$,
594 again higher than values suggested by this study (e.g. $62 \text{ eq ha}^{-1} \text{ yr}^{-1}$ in Saskatchewan). In comparison to these
595 empirical values, $CL_{nut}N$ values in the current work are lower by a factor of 2. If $CL_{nut}N$ is doubled, only 10% of the
596 soils assessed are in exceedance (versus 31% of soils). This reduction in the areal exceedance would in turn reduce
597 the number of PA and OECM sites in exceedance. While the spatial pattern of $CL_{nut}N$ exceedances does not
598 generally follow exceedances of critical loads of acidity, some areas (including PA and OECM sites) in central
599 Canada were estimated to be in exceedance of both critical loads of acidity and nutrient N, suggesting that this

600 region may be of particular concern. Given the largest areal exceedance is of $CL_{min}N$, observational studies with the
601 view of expanding Canadian ecosystem empirical critical loads would help determine how, and by how much,
602 Canadian ecosystems are affected by N_{dep} and how well these observations align with $CL_{min}N$ in the current work.
603 Additionally, vegetation community changepoint modelling such with the TITAN model (Baker, 2010) could help
604 bring understanding to how Canadian ecosystems might experience elevated N_{dep} with regard to changes in
605 biodiversity. Widespread $CL_{min}N$ exceedance (found in the majority of the PA and OECM sites assessed) suggests that
606 nutrient N may present a risk to biodiversity at many sites under protective measures. While some empirical studies
607 of nutrient N have been done in Canada, a large knowledge gap exists for many Canadian ecosystems regarding the
608 effect of nutrient nitrogen and their critical loads. Some work has developed on Jack Pine and northern ecosystems;
609 Vandinter suggested that across Jack pine dominant forests surrounding the AOSR, the biodiversity-based
610 empirical critical load of nutrient N was $5.6 \text{ kg ha}^{-1} \text{ yr}^{-1}$ ($400 \text{ eq ha}^{-1} \text{ yr}^{-1}$; Vandinter and Aherne, 2023a) which is
611 above the maximum $CL_{min}N$ calculated in this study within 200 km of the AOSR ($216 \text{ eq ha}^{-1} \text{ yr}^{-1}$). Further, in low
612 deposition 'background' regions a biodiversity-based empirical critical load of $1.4\text{--}3.15 \text{ kg ha}^{-1} \text{ yr}^{-1}$ ($100\text{--}225 \text{ eq}$
613 $\text{ha}^{-1} \text{ yr}^{-1}$) was found to protect lichen communities and other N-sensitive species in Jack pine forests across
614 Northwestern Canada (Vandinter and Aherne, 2023b); these are again higher compared to mean values in this
615 study (e.g. for the Boreal Plain, $76 \text{ eq ha}^{-1} \text{ yr}^{-1}$). Empirical critical loads developed for ecoregions in Northern
616 Saskatchewan (Murray et al., 2017) fall into a range of $88\text{--}123 \text{ eq ha}^{-1} \text{ yr}^{-1}$, again higher than values suggested by
617 this study (e.g. $62 \text{ eq ha}^{-1} \text{ yr}^{-1}$ in Saskatchewan). While the spatial pattern of $CL_{min}N$ exceedances does not generally
618 follow exceedances of critical loads of acidity, some areas (including PA and OECM sites) in central Canada were
619 estimated to be in exceedance of both critical loads of acidity and nutrient N, suggesting that this region may be of
620 particular concern.

622 5 Conclusions

623 This study mapped critical loads of acidity and nutrient nitrogen for terrestrial ecosystems the using the steady-state
624 SMB model. The modelling approach used (a) high-resolution national maps of soils, meteorology, and forest
625 composition, (b) high-resolution modelled Canada-wide B_{Cdep} , and (c) species-specific chemical criteria for damage.
626 The resulting national critical loads of acidity and nutrient N for Canadian terrestrial ecosystems were mapped at a
627 250 m resolution. The influence of different levels of protection and B_{Cdep} models ~~to several parameters~~ was also
628 explored, including two vegetation protection levels (5% and 20% root biomass growth reduction scenarios) and
629 anthropogenic base cation deposition "hot spots".

630
631 Terrestrial ecosystems in Canada continue to receive acidic deposition in excess of their critical loads for both
632 acidity and nutrient N under modelled (2014–2016 average) total S and N deposition in areas of both eastern and
633 western Canada. These areas include several major point emissions sources including the Alberta Oil Sands Region.
634 Further, exceedance was predicted at 10% (acidity) and 70% (nutrient nitrogen) of the assessed sites (PA and
635 OECM) where preserving biodiversity is a national policy goal, suggesting that current levels of N deposition may

636 be affecting a large majority of these ecologically important sites. Soil recovery from acidic deposition is a slow
637 process that may take decades or even centuries to reach pre-acidification levels, which cannot begin until
638 deposition falls below critical loads. Parameterization of the SMB model specifically for Canadian ecosystems is a
639 step forward in refining Canadian terrestrial critical loads, and the maps produced by this study are a valuable tool in
640 identifying and assessing regions sensitive to acidic deposition and nutrient N deposition, as well ~~they provide~~
641 providing a foundation for more refined provincial estimates.

642 **CRedit authorship contribution statement**

643 **H. Cathcart:** Conceptualization, Data curation, Investigation, Methodology, Formal analysis, Visualization, Writing
644 – original draft, Writing – review & editing. **J. Aherne:** Formal analysis, Methodology, Writing – review &
645 editing. **M.D. Moran:** Data curation, Investigation, Methodology, Writing – original draft, Writing – review &
646 editing. **V. Savic-Jovicic:** Data curation, Investigation. **P.A. Makar:** Investigation, Methodology, Writing – original
647 draft, Writing – review & editing. **A.D Cole:** Writing – review & editing.

648 **Competing interests**

649 The authors declare that they have no conflict of interest.

650 **Data availability**

651 Raster files of critical load maps (CL_{maxS} , CL_{maxN} , CL_{minN} , CL_{nutN}) will be made available on the Government of
652 Canada's Open Data Portal under Environment and Climate Change Canada's records
653 (<https://open.canada.ca/data/organization/ec>) at <https://doi.org/10.18164/ec5c8bbb-3bc8-4675-a9c6-103add874b8>.

654 **Acknowledgements**

655 This study was funded by Environment and Climate Change Canada. The authors wish to acknowledge Max Posch
656 for his provision of (and guidance regarding) soil water runoff (Q) estimates, and the AQMEI4 project for
657 emissions data leading to GEM-MACH maps of base cation deposition.

658 **Copyright**

659 The works published in this journal are distributed under the Creative Commons Attribution 4.0 License. This
660 licence does not affect the Crown copyright work.

661
662 © His Majesty the King in Right of Canada, as represented by the Minister of Environment and Climate Change
663 Canada, 2024.

664 **References**

- 665 Agriculture and Agri-Food Canada: Terrestrial Ecozones of Canada [dataset], <https://open.canada.ca/data/en/dataset/7ad7ea01-eb23-4824-bccc-66adb7c5bd8>, 2013.
- 666
- 667 Aherne, J. and Posch, M.: Impacts of nitrogen and sulphur deposition on forest ecosystem services in Canada, *Curr. Opin. Environ. Sustain.*, 5, 108–115, <https://doi.org/10.1016/j.cosust.2013.02.005>, 2013.
- 668
- 669 Akilu, Y.-A., Blair, L., Dinwoodie, G., and Aherne, J.: Using steady-state mass balance model to determine critical loads of acidity for terrestrial ecosystems in Alberta, Government of Alberta, Ministry of Environment and Parks, 2022.
- 670
- 671 [Baker, M. E. and King, R. S.: A new method for detecting and interpreting biodiversity and ecological community thresholds, *Methods Ecol. Evol.*, 1, 25–37, <https://doi.org/10.1111/j.2041-210X.2009.00007.x>, 2010.](#)
- 672
- 673 Beaudoin, A., Bernier, P. Y., Guindon, L., Villemare, P., Guo, X. J., Stinson, G., Bergeron, T., Magnussen, S., and Hall, R. J.: Mapping attributes of Canada's forests at moderate resolution through kNN and MODIS imagery, *Can. J. For. Res.*, 44, 521–532, <https://doi.org/10.1139/cjfr-2013-0401>, 2014.
- 674
- 675
- 676 Bobbink, R. and Hicks, W. K.: Factors Affecting Nitrogen Deposition Impacts on Biodiversity: An Overview, in: Nitrogen Deposition, Critical Loads and Biodiversity, edited by: Sutton, M. A., Mason, K. E., Sheppard, L. J., Sverdrup, H., Haeuber, R., and Hicks, W. K., Springer Netherlands, Dordrecht, 127–138, https://doi.org/10.1007/978-94-007-7939-6_14, 2014.
- 677
- 678
- 679 Bobbink, R., Loran, C., and Tomassen, H.: Review and revision of empirical critical loads of nitrogen for Europe, Umweltbundesamt/German Environment Agency, Dessau-Roßlau, Germany, 2022.
- 680
- 681 Bonten, L. T. C., Reinds, G. J., and Posch, M.: A model to calculate effects of atmospheric deposition on soil acidification, eutrophication and carbon sequestration, *Environ. Model. Softw.*, 79, 75–84, <https://doi.org/10.1016/j.envsoft.2016.01.009>, 2016.
- 682
- 683 Boutzis, E. I., Zhang, J., and Moran, M. D.: Expansion of a size disaggregation profile library for particulate matter emissions processing from three generic profiles to 36 source-type-specific profiles, *J. Air Waste Manag. Assoc.*, 70, 1067–1100, <https://doi.org/10.1080/10962247.2020.1743794>, 2020.
- 684
- 685
- 686 Bouwman, A. F., Vuuren, D. P. V., Derwent, R. G., and Posch, M.: A Global Analysis of Acidification and Eutrophication of Terrestrial Ecosystems, *Water, Air, Soil Pollut.*, 141, 349–382, <https://doi.org/10.1023/A:1021398008726>, 2002.
- 687
- 688 Bullard, J. E., Baddock, M., Bradwell, T., Crusius, J., Darlington, E., Gaiero, D., Gassó, S., Gisladottir, G., Hodgkins, R., McCulloch, R., McKenna-Neuman, C., Mockford, T., Stewart, H., and Thorsteinsson, T.: High-latitude dust in the Earth system, *Rev. Geophys.*, 54, 447–485, <https://doi.org/10.1002/2016RG000518>, 2016.
- 689
- 690
- 691 Burns, D. A., Blett, T., Haeuber, R., and Pardo, L. H.: Critical loads as a policy tool for protecting ecosystems from the effects of air pollutants, *Front. Ecol. Environ.*, 6, 156–159, <https://doi.org/10.1890/070040>, 2008.
- 692
- 693 Carou, S., Dennis, I., Aherne, J., Ouimet, R., Arp, P. A., Watmough, S. A., DeMerchant, I., Shaw, M., Vet, B., Bouchet, V., and Moran, M.: A national picture of acid deposition critical loads for forest soils in Canada, Canadian Council of Ministers of the Environment, Winnipeg, Manitoba, 2008.
- 694
- 695
- 696 Cathcart, H., Aherne, J., Jeffries, D. S., and Scott, K. A.: Critical loads of acidity for 90,000 lakes in northern Saskatchewan: A novel approach for mapping regional sensitivity to acidic deposition, *Atmos. Environ.*, 146, 290–299, <https://doi.org/10.1016/j.atmosenv.2016.08.048>, 2016.
- 697
- 698
- 699 CEC: 2010 Land Cover of North America at 250 meters (v2.0) [dataset], Commission for Environmental Cooperation (CEC).
- 700 Canada Centre for Remote Sensing (CCRS), U.S. Geological Survey (USGS), Comisión Nacional para el Conocimiento y Uso de la Biodiversidad (CONABIO), Comisión Nacional Forestal (CONAFOR), Instituto Nacional de Estadística y Geografía (INEGI), <http://www.cec.org/north-american-environmental-atlas/land-cover-2010-modis-250m>, 2018.
- 701
- 702
- 703 Chen, J., Anderson, K., Pavlovic, R., Moran, M. D., Englefield, P., Thompson, D. K., Munoz-Alpizar, R., and Landry, H.: The FireWork v2.0 air quality forecast system with biomass burning emissions from the Canadian Forest Fire Emissions Prediction System v2.03, *Geosci. Model Dev.*, 12, 3283–3310, <https://doi.org/10.5194/gmd-12-3283-2019>, 2019.
- 704
- 705

706 Clark, C. M., Morefield, P. E., Gilliam, F. S., and Pardo, L. H.: Estimated losses of plant biodiversity in the United States from
707 historical N deposition (1985–2010), *Ecology*, 94, 1441–1448, <https://doi.org/10.1890/12-2016.1>, 2013.

708 CLBBR: Soil Landscapes of Canada, v. 2.2 [dataset], Centre for Land and Biological Resources Research. Research Branch,
709 Agriculture and Agri-Food Canada, <https://sis.agr.gc.ca/cansis/nsdb/slc/v2.2>, 1996.

710 CLRTAP: Mapping critical loads for ecosystems, Chapter V of Manual on methodologies and criteria for modelling and mapping
711 critical loads and levels and air pollution effects, risks and trends. UNECE Convention on Long-range Transboundary Air
712 Pollution, ~~accessed 09/16/2024~~ at www.icpmapping.org, 2015.

713 Cronan, C. S. and Schofield, C. L.: Relationships between aqueous aluminum and acidic deposition in forested watersheds of
714 North America and northern Europe, *Environ. Sci. Technol.*, 24, 1100–1105, <https://doi.org/10.1021/es00077a022>, 1990.

715 ~~De Vries, W., Posch, M., Reinds, G. J., and Kämäri, J.: Critical loads and their exceedance on forest soils in Europe, Report - The~~
716 ~~Winand Staring Centre for Integrated Land, Soil and Water Research (SC-DLO), Wageningen, the Netherlands, 123 pp., 1992.~~

717 De Vries, W., Hettelingh, J.-P., and Posch, M. (Eds.): The History and Current State of Critical Loads and Dynamic Modelling
718 Assessments, in: Critical loads and dynamic risk assessments: Nitrogen, acidity and metals in terrestrial and aquatic ecosystems,
719 Springer, 1–11, https://doi.org/10.1007/978-94-017-9508-1_1, 2015.

720 Dymond, C. C., Titus, B. D., Stinson, G., and Kurz, W. A.: Future quantities and spatial distribution of harvesting residue and
721 dead wood from natural disturbances in Canada, *For. Ecol. Manag.*, 260, 181–192, <https://doi.org/10.1016/j.foreco.2010.04.015>,
722 2010.

723 ECCC: Evaluation of the Addressing Air Pollution Horizontal Initiative, Environment and Climate Change Canada, ISBN: 978-
724 0-660-39645-3, 2021.

725 ~~ECCC: Canadian Environmental Sustainability Indicators: Extent of Canada's Wetlands, ISBN: 978-0-660-05390-5, 2016.~~

726 ECCC: 2022 Canadian Protected and Conserved Areas Database (CPCAD) User Manual, ~~Environ. Clim. Change~~
727 ~~Canada/Environment and Climate Change Canada~~, [https://data-donnees.ec.gc.ca/data/species/protectrestore/canadian-protected-
728 conserved-areas-database/ProtectedConservedAreaUserManual.pdf](https://data-donnees.ec.gc.ca/data/species/protectrestore/canadian-protected-conserved-areas-database/ProtectedConservedAreaUserManual.pdf), 2023a.

729 ECCC: Canadian Protected and Conserved Areas Database 2022 [dataset], Environment and Climate Change Canada,
730 <https://www.canada.ca/en/environment-climate-change/services/national-wildlife-areas/protected-conserved-areas-database.html>,
731 2023b.

732 ECCC: Toward a 2030 Biodiversity Strategy- for Canada: Halting and ~~reversing-Reversing nature-Nature lossLoss~~, Environment
733 and Climate Change Canada, ISBN: 978-0-660-48594-2, 2023c.

734 ECCC: Canada's air pollutant emissions inventory report 1990-2022., Environment and Climate Change Canada. ISSN: 2562-
735 4903. https://publications.gc.ca/collections/collection_2024/eccc/En81-30-2022-eng.pdf, Gatineau, Quebec, 2024.

736 ~~FAO-UNESCO: Digital soil map of the world and derived soil properties, CD-ROM, Rome, Rome-FAO-, ISBN: 978-92-3-~~
737 ~~103889-1, 92-3-103889-3, 2003.~~

738 Feng, J., Vet, R., Cole, A., Zhang, L., Cheng, I., O'Brien, J., and Macdonald, A.-M.: Inorganic chemical components in
739 precipitation in the eastern U.S. and Eastern Canada during 1989–2016: Temporal and regional trends of wet concentration and
740 wet deposition from the NADP and CAPMoN measurements, *Atmos. Environ.*, 254, 118367,
741 <https://doi.org/10.1016/j.atmosenv.2021.118367>, 2021.

742 Forsius, M., Posch, M., Aherne, J., Reinds, G., Christensen, J., and Hole, L.: Assessing the Impacts of Long-Range Sulfur and
743 Nitrogen Deposition on Arctic and Sub-Arctic Ecosystems, *Ambio*, 39, 136–47, <https://doi.org/10.1007/s13280-010-0022-7>,
744 2010.

745 Galmarini, S., Makar, P., Clifton, O. E., Hogrefe, C., Bash, J. O., Bellasio, R., Bianconi, R., Bieser, J., Butler, T., Ducker, J.,
746 Flemming, J., Hodzic, A., Holmes, C. D., Kioutsioukis, I., Kranenburg, R., Lupascu, A., Perez-Camanyo, J. L., Pleim, J., Ryu,
747 Y.-H., San Jose, R., Schwede, D., Silva, S., and Wolke, R.: Technical note: AQMEII4 Activity 1: evaluation of wet and dry
748 deposition schemes as an integral part of regional-scale air quality models, *Atmospheric Chem. Phys.*, 21, 15663–15697,
749 <https://doi.org/10.5194/acp-21-15663-2021>, 2021.

750 Hazlett, P., Emilson, C., Lawrence, G., Fernandez, I., Ouimet, R., and Bailey, S.: Reversal of Forest Soil Acidification in the
751 Northeastern United States and Eastern Canada: Site and Soil Factors Contributing to Recovery, *Soil Syst.*, 4, 54,
752 <https://doi.org/10.3390/soilsystems4030054>, 2020.

753 Hengl, T.: SoilGrids250m 2017-03 Absolute depth to bedrock (in cm). [dataset], ISRIC - World Soil Inf.,
754 <https://data.isric.org/geonetwork/srv/api/records/f36117ea-9be5-4afd-bb7d-7a3e77bf392a>, 2017.

755 Hengl, T.: Clay content in % (kg / kg) at 6 standard depths (0, 10, 30, 60, 100 and 200 cm) at 250 m resolution (v0.2). [dataset],
756 Zenodo, <https://doi.org/10.5281/zenodo.2525663>, 2018a.

757 Hengl, T.: Coarse fragments % (volumetric) at 6 standard depths (0, 10, 30, 60, 100 and 200 cm) at 250 m resolution [dataset],
758 <https://doi.org/10.5281/zenodo.2525682>, 2018b.

759 Hengl, T.: Sand content in % (kg / kg) at 6 standard depths (0, 10, 30, 60, 100 and 200 cm) at 250 m resolution (v0.2) [dataset],
760 Zenodo, <https://doi.org/10.5281/zenodo.2525662>, 2018c.

761 Hengl, T.: Soil bulk density (fine earth) 10 x kg / m-cubic at 6 standard depths (0, 10, 30, 60, 100 and 200 cm) at 250 m
762 resolution (v0.2) [dataset], Zenodo, <https://doi.org/10.5281/zenodo.2525665>, 2018d.

763 Hengl, T. and Wheeler, I.: Soil organic carbon content in x 5 g / kg at 6 standard depths (0, 10, 30, 60, 100 and 200 cm) at 250 m
764 resolution (v0.2) [dataset], Zenodo, <https://doi.org/10.5281/zenodo.2525553>, 2018.

765 [Hijmans, R.J.: terra: Spatial Data Analysis. R package version 1.7-23](https://CRAN.R-project.org/package=terra), <https://CRAN.R-project.org/package=terra>, 2023.

766 [Johnson, Dale W., and John Turner: Nitrogen budgets of forest ecosystems: a review. Forest Ecology and Management 318,370-379](https://doi.org/10.1016/j.foreco.2013.08.028), <https://doi.org/10.1016/j.foreco.2013.08.028>, 2014.

767

768 Koseva, I. S., Watmough, S. A., and Aherne, J.: Estimating base cation weathering rates in Canadian forest soils using a simple
769 texture-based model, *Biogeochemistry*, 101, 183–196, <https://doi.org/10.1007/s10533-010-9506-6>, 2010.

770 Lawrence, G. B., David, M. B., Lovett, G. M., Murdoch, P. S., Burns, D. A., Stoddard, J. L., Baldigo, B. P., Porter, J. H., and
771 Thompson, A. W.: Soil Calcium Status and the Response of Stream Chemistry to Changing Acidic Deposition Rates, *Ecol.*
772 *Appl.*, 9, 1059–1072, [https://doi.org/10.1890/1051-0761\(1999\)009\[1059:SCSATR\]2.0.CO;2](https://doi.org/10.1890/1051-0761(1999)009[1059:SCSATR]2.0.CO;2), 1999.

773 Lawrence, G. B., Hazlett, P. W., Fernandez, I. J., Ouimet, R., Bailey, S. W., Shortle, W. C., Smith, K. T., and Antidormi, M. R.:
774 Declining Acidic Deposition Begins Reversal of Forest-Soil Acidification in the Northeastern U.S. and Eastern Canada, *Environ.*
775 *Sci. Technol.*, 49, 13103–13111, <https://doi.org/10.1021/acs.est.5b02904>, 2015.

776 Li, H. and McNulty, S. G.: Uncertainty analysis on simple mass balance model to calculate critical loads for soil acidity, *Environ.*
777 *Pollut.*, 149, 315–26, <https://doi.org/10.1016/j.envpol.2007.05.014>, 2007.

778 Liang, T. and Aherne, J.: Critical loads of acidity and exceedances for 1138 lakes and ponds in the Canadian Arctic, *Sci. Total*
779 *Environ.*, 652, 1424–1434, <https://doi.org/10.1016/j.scitotenv.2018.10.330>, 2019.

780 Likens, G. E., Driscoll, C. T., and Buso, D. C.: Long-term effects of acid rain: response and recovery of a forest ecosystem,
781 *Science*, 272, 244–246, <https://doi.org/10.1126/science.272.5259.244>, 1996.

782 Makar, P. A., Akingunola, A., Aherne, J., Cole, A. S., Aklilu, Y., Zhang, J., Wong, I., Hayden, K., Li, S.-M., Kirk, J., Scott, K.,
783 Moran, M. D., Robichaud, A., Cathcart, H., Baratzedah, P., Pabla, B., Cheung, P., Zheng, Q., and Jeffries, D. S.: Estimates of
784 exceedances of critical loads for acidifying deposition in Alberta and Saskatchewan, *Atmospheric Chem. Phys.*, 18, 9897–9927,
785 <https://doi.org/10.5194/acp-18-9897-2018>, 2018.

786 [Mandre, M., Kask, R., Pikk, J., and Ots, K.: Assessment of growth and stemwood quality of Scots pine on territory influenced by alkaline industrial dust, Environ. Monit. Assess., 138, 51–63](https://doi.org/10.1007/s10661-007-9790-3), <https://doi.org/10.1007/s10661-007-9790-3>, 2008.

787

788 McDonnell, T. C., Phelan, J., Talhelm, A. F., Cosby, B. J., Driscoll, C. T., Sullivan, T. J., and Greaver, T.: Protection of forest
789 ecosystems in the eastern United States from elevated atmospheric deposition of sulfur and nitrogen: A comparison of steady-
790 state and dynamic model results, *Environ. Pollut.*, 318, 120887, <https://doi.org/10.1016/j.envpol.2022.120887>, 2023.

791 McKenney, D., Papadopol, P., Campbell, K., Lawrence, K., Hutchinson, M., and others: Spatial models of Canada and North
792 America-wide 1971/2000 minimum and maximum temperature, total precipitation and derived bioclimatic variables. *Frontline*
793 *Technical Note* 106., 2006.

794 Mongeon, A., Aherne, J., and Watmough, S. A.: Steady-state critical loads of acidity for forest soils in the Georgia Basin, British
795 Columbia, *J. Limnol.*, 69, 193–200, <https://doi.org/10.4081/jlimnol.2010.s1.193>, 2010.

796 Moran, M. D., Savic-Jovcic, V., Makar, P. A., Gong, W., Stroud, C. A., Zhang, J., Zheng, Q., Chen, J., Akingunola, A., Lupu, A.,
797 Ménard, S., Menelaou, K., and Munoz-Alpizar, R.: Operational chemical weather forecasting with the ECCO online Regional Air
798 Quality Deterministic Prediction System version 023 (RAQDPS023) - Part 1: System description, *Geosci Model Dev Prep.*,
799 2024a.

800 Moran, M. D., Lupu, A., Savic-Jovcic, V., Zhang, J., Zheng, Q., Boutzis, E., Mashayekhi, R., Stroud, C. A., Ménard, S., Chen, J.,
801 Menelaou, K., Munoz-Alpizar, R., Koric, D., and Manseau, P.: Operational chemical weather forecasting with the ECCO online
802 Regional Air Quality Deterministic Prediction System version 023 (RAQDPS023) - Part 2: Prospective and retrospective
803 performance evaluations, *Geosci Model Dev Prep.*, 2024b.

804 Murray, C. A., Whitfield, C. J., and Watmough, S. A.: Uncertainty-based terrestrial critical loads of nutrient nitrogen in northern
805 Saskatchewan, Canada, *Boreal Environ. Res.*, 22, 4(1-6), 2017.

806 [Myers-Smith, I.H., Kerby, J.T., Phoenix, G.K. et al: Complexity revealed in the greening of the Arctic. *Nat. Clim. Chang.* 10,
807 106–117, <https://doi.org/10.1038/s41558-019-0688-1>, 2020.](https://doi.org/10.1038/s41558-019-0688-1)

808 NADP: National Trends Network [dataset], National Atmospheric Deposition Program (NRSP-3). NADP Program Office,
809 Wisconsin State Laboratory of Hygiene, 465 Henry Mall, Madison, WI 53706, <https://nadp.slh.wisc.edu/networks/national-trends-network>, 2023.

811 [National Wetlands Working Group: The Canadian Wetland Classification System, 2nd ed, edited by: Warner, B.G., Rubec,
812 C.D.A., National Wetlands Working Group, Wetlands Research Branch, University of Waterloo, Waterloo, ON, Canada, 1997.](https://www.ec.gc.ca/nwet/14889617-9033-4980-b068-641c34bd881e)

813 NEG-ECP: Critical Load of Sulphur and Nitrogen Assessment and Mapping Protocol for Upland Forests, N. Engl. Gov. East.
814 Can. Prem. Environ. Task Group Acid Rain Action Plan Halifax N. S., 2001.

815 Nilsson, J. and Grenfelt, P.: Critical ~~levels~~ loads for sulphur and nitrogen, ~~418 pp.~~ *Nord-ic Council of Ministers,*
816 *CphCopenhagen, Denmark*, 1988.

817 Ouimet, R., Duchesne, L., Houle, D., and Arp, P.: Critical Loads and Exceedances of Acid Deposition and Associated Forest
818 Growth in the Northern Hardwood and Boreal Coniferous Forests in Québec, Canada, *Water Air Soil Pollut. Focus*, 1, 119–134,
819 <https://doi.org/10.1023/A:1011544325004>, 2001.

820 Ouimet, R., Arp, P. A., Watmough, S. A., Aherne, J., and DeMerchant, I.: Determination and Mapping Critical Loads of Acidity
821 and Exceedances for Upland Forest Soils in Eastern Canada, *Water. Air. Soil Pollut.*, 172, 57–66, <https://doi.org/10.1007/s11270-005-9050-5>, 2006.

823 [Paal, J., Degtjarenko, P., Suija, A., and Liira, J.: Vegetation responses to long-term alkaline cement dust pollution in inus
824 sylvestris-dominated boreal forests – niche breadth along the soil pH gradient, *Appl. Veg. Sci.*, 16, 248–259,
825 <https://doi.org/10.1111/j.1654-109X.2012.01224.x>, 2013.](https://doi.org/10.1111/j.1654-109X.2012.01224.x)

826 Pardo, L. H., Duarte, N., Miller, E. K., and Robin-Abbott, M.: Tree chemistry database (version 1.0), USDA For. Serv.
827 Northeast. Res. Stn., 324, <https://doi.org/10.2737/NE-GTR-324>, 2005.

828 Pardo, L. H., Coombs, J. A., Robin-Abbott, M. J., Pontius, J. H., and D'Amato, A. W.: Tree species at risk from nitrogen
829 deposition in the northeastern United States: A geospatial analysis of effects of multiple stressors using exceedance of critical
830 loads, *For. Ecol. Manag.*, 454, 117528, <https://doi.org/10.1016/j.foreco.2019.117528>, 2019.

831 Paré, D., Bernier, P., Lafleur, B., Titus, B. D., Thiffault, E., Maynard, D. G., and Guo, X.: Estimating stand-scale biomass,
832 nutrient contents, and associated uncertainties for tree species of Canadian forests, *Can. J. For. Res.*, 43, 599–608,
833 <https://doi.org/10.1139/cjfr-2012-0454>, 2013.

834 Park, S. H., Gong, S. L., Gong, W., Makar, P. A., Moran, M. D., Zhang, J., and Stroud, C. A.: Relative impact of windblown dust
835 versus anthropogenic fugitive dust in PM_{2.5} on air quality in North America, *J. Geophys. Res. Atmospheres*, 115,
836 <https://doi.org/10.1029/2009JD013144>, 2010.

837 Posch, M., de Smet, P. A. M., Hettelingh, J.-P., and Downing, R. J.: Calculation and Mapping of Critical Thresholds in Europe:
838 Status Report 1999, Coordination Center for Effects, National Institute of Public Health and the Environment, Bilthoven,
839 Netherlands, 1999.

840 Posch, M., de Vries, W., and Sverdrup, H. U.: Mass Balance Models to Derive Critical Loads of Nitrogen and Acidity for
841 Terrestrial and Aquatic Ecosystems, in: *Critical Loads and Dynamic Risk Assessments: Nitrogen, Acidity and Metals in*
842 *Terrestrial and Aquatic Ecosystems*, edited by: de Vries, W., Hettelingh, J.-P., and Posch, M., Springer Netherlands, Dordrecht,
843 171–205, https://doi.org/10.1007/978-94-017-9508-1_6, 2015.

844 Pribyl, D. W.: A critical review of the conventional SOC to SOM conversion factor, *Geoderma*, 156, 75–83,
845 <https://doi.org/10.1016/j.geoderma.2010.02.003>, 2010.

846 [QGIS Development Team: QGIS Geographic Information System, Open Source Geospatial Foundation](http://qgis.osgeo.org)
847 [Project, http://qgis.osgeo.org, 2023.](http://qgis.osgeo.org) [QGIS Development Team: QGIS Geographic Information System, QGIS Association, 2023.](https://www.qgis.org/en/about/association/)

848 [R Core Team: R: A Language and Environment for Statistical Computing, version 4.1.0, R Foundation for Statistical Computing,](https://www.r-project.org/)
849 [Vienna, Austria, 2021.](https://www.r-project.org/)

850 Radke, L., Hegg, D., Lyons, J., Brock, C., Hobbs, P., Weiss, R., and Rasmussen, R.: Airborne measurements on smokes from
851 biomass burning, *Aerosols Clim.*, 411–422, 1988.

852 Radke, L. F., Lyons, J. H., Hobbs, P. V., Hegg, D. A., Sandberg, D. V., and Ward, D. E.: Airborne monitoring and smoke
853 characterization of prescribed fires on forest lands in western Washington and Oregon, US Department of Agriculture, Forest
854 Service, Pacific Northwest Research Station, 1990.

855 Reinds, G. J., Posch, M., Aherne, J., and Forsius, M.: Assessment of Critical Loads of Sulphur and Nitrogen and Their
856 Exceedances for Terrestrial Ecosystems in the Northern Hemisphere, in: *Critical loads and dynamic risk assessments: Nitrogen,*
857 *acidity and metals in terrestrial and aquatic ecosystems*, edited by: De Vries, W., Hettelingh, J.-P., and Posch, M., Springer, 403–
858 418, https://doi.org/10.1007/978-94-017-9508-1_15, 2015.

859 Reinds, G. J., Thomas, D., Posch, M., and Slootweg, J.: Critical loads for eutrophication and acidification for European terrestrial
860 ecosystems, Umweltbundesamt, Wörlitzer Platz 1, 06844 Dessau-Roßlau, Germany, 2021.

861 Rosen, K., Gundersen, P., Tegnhammar, L., Johansson, M., and Frogner, T.: Nitrogen enrichment of Nordic forest ecosystems:
862 the concept of critical loads, *Ambio*, 21:5, 364–368, 1992.

863 Shangguan, W., Hengl, T., Mendes de Jesus, J., Yuan, H., and Dai, Y.: Mapping the global depth to bedrock for land surface
864 modeling, *J. Adv. Model. Earth Syst.*, 9, 65–88, <https://doi.org/10.1002/2016MS000686>, 2017.

865 Simkin, S. M., Allen, E. B., Bowman, W. D., Clark, C. M., Belnap, J., Brooks, M. L., Cade, B. S., Collins, S. L., Geiser, L. H.,
866 Gilliam, F. S., Jovan, S. E., Pardo, L. H., Schulz, B. K., Stevens, C. J., Suding, K. N., Throop, H. L., and Waller, D. M.:
867 Conditional vulnerability of plant diversity to atmospheric nitrogen deposition across the United States, *Proc. Natl. Acad. Sci.*,
868 113, 4086–4091, <https://doi.org/10.1073/pnas.1515241113>, 2016.

869 Skeffington, R., Whitehead, P., and Abbott, J.: Quantifying uncertainty in critical loads: (B) Acidity mass balance critical loads
870 on a sensitive site, *Water. Air. Soil Pollut.*, 169, 25–46, <https://doi.org/10.1007/s11270-006-2218-9>, 2006.

871 SLCWG: Soil landscapes of Canada version 3.2 [dataset], Soil Landscapes of Canada Working Group. Agriculture and Agri-
872 Food Canada, <https://sis.agr.gc.ca/cansis/nsdb/slc/v3.2/index.html>, 2010.

873 Statistics Canada: Agricultural ecumene boundary file, 2016 Census of Agriculture [dataset], Statistics Canada, Cat. No 92-639-
874 X, <https://www150.statcan.gc.ca/>, 2017.

875 Sverdrup, H. and De Vries, W.: Calculating critical loads for acidity with the simple mass balance method, *Water. Air. Soil*
876 *Pollut.*, 72, 143–162, <https://doi.org/10.1007/BF01257121>, 1994.

- 877 Sverdrup, H. and Warfvinge, P.: The effect of soil acidification effect on the growth of trees, grass and herbs, as expressed by the
878 $(Ca+ Mg+ K)/Al/Al$ ratio, Reports in ecology and environmental engineering, Lund University Department of Chemical
879 Engineering II, 1993.
- 880 Tegen, I. and Fung, I.: Contribution to the atmospheric mineral aerosol load from land surface modification, *J. Geophys. Res.*
881 *Atmospheres*, 100, 18707–18726, <https://doi.org/10.1029/95JD02051>, 1995.
- 882 Tol, P.: Colour schemes, SRON Technical Note, Doc. no. SRON/EPS/TN/09-002, [https://personal.sron.nl/pault/colourschemes.](https://personal.sron.nl/pault/colourschemes.pdf)
883 pdf, 2012.
- 884 Vandinther, N. and Aherne, J.: Biodiversity-Based Empirical Critical Loads of Nitrogen Deposition in the Athabasca Oil Sands
885 Region, *Nitrogen*, 4, 169–193, <https://doi.org/10.3390/nitrogen4020012>, 2023a.
- 886 Vandinther, N. and Aherne, J.: Ecological Risks from Atmospheric Deposition of Nitrogen and Sulphur in Jack Pine forests of
887 Northwestern Canada, *Nitrogen*, 4, 102–124, <https://doi.org/10.3390/nitrogen4010008>, 2023b.
- 888 ~~de Vries, W., Posch, M., Reinds, G. J., and Kämäri, J.: Critical loads and their exceedance on forest soils in Europe, Report—The~~
889 ~~Winand Staring Centre for Integrated Land, Soil and Water Research (SC-DLO), Wageningen, the Netherlands, 123 pp., 1992-~~
- 890 Whitfield, C. J., Aherne, J., Watmough, S. A., and ~~McDONALD~~McDonald, M.: Estimating the sensitivity of forest soils to acid
891 deposition in the Athabasca Oil Sands Region, Alberta, *J. Limnol.*, 69, 201, <https://doi.org/10.4081/jlimnol.2010.s1.201>, 2010.
- 892 Wilkins, K., Cathcart, H., Hickey, P., Hanley, O., Vintró, L. L., and Aherne, J.: Influence of Precipitation on the Spatial
893 Distribution of 210Pb, 7Be, 40K and 137Cs in Moss, *Pollutants*, 3, 102–113, <https://doi.org/10.3390/pollutants3010009>, 2023.
- 894 Williston, P., Aherne, J., Watmough, S., Marmorek, D., Hall, A., de la Cueva Bueno, P., Murray, C., Henolson, A., and
895 Laurence, J. A.: Critical levels and loads and the regulation of industrial emissions in northwest British Columbia, Canada,
896 *Atmos. Environ.*, 146, 311–323, <https://doi.org/10.1016/j.atmosenv.2016.08.058>, 2016.
- 897 Wu, W. and Driscoll, C. T.: Impact of Climate Change on Three-Dimensional Dynamic Critical Load Functions, *Environ. Sci.*
898 *Technol.*, 44, 720–726, <https://doi.org/10.1021/es900890t>, 2010.
- 899 Zhao, W., Zhao, Y., Ma, M., Chang, M., and Duan, L.: Long-term variability in base cation, sulfur and nitrogen deposition and
900 critical load exceedance of terrestrial ecosystems in China, *Environ. Pollut.*, 289, 117974,
901 <https://doi.org/10.1016/j.envpol.2021.117974>, 2021.

902